Supporting Material for "*Higher temperature extremes exacerbate negative disease effects in a social mammal*"

Questions and inquiries can be sent to the corresponding author, Maria Paniw, at m.paniw@gmail.ocm or maria.paniw@ebd.csic.es

We note that all data and code to build and project the IBM are deposited on Zenodo https://doi.org/10.5281/zenodo.5784649; see also https://github.com/MariaPaniw/IBM_meerkat.

Table of Contents

Supporting Material S1 – Meerkat demography

S1.1 Meerkat life history data

The harsh climate of the Kalahari, characterized by seasonal variation and high interannual unpredictability in weather patterns[1], is believed to have favoured the evolution of obligate cooperative breeding in meerkats[2–4]. A dominant female monopolizes breeding and, when pregnant, typically evicts pregnant subordinate female helpers[5–7]. Evicted females typically return to the group within a month but are evicted again in successive breeding attempts. Evicted females can emigrate and form new groups, and their decision to emigrate is strongly influenced by social cues[8]. Female immigration into an existing social group is extremely rare[9] (ED Fig. 2). Males, both dominants and subordinates, frequently emigrate from groups to join evicted females, and males also immigrate into a group to gain reproductive opportunities. Dominant females can produce up to four litters per year, each of 2-6 pups[6]. Reproduction is usually confined to the period between August and April, peaking in January, when temperatures are highest and rainfall is abundant (most rain falls Feb-Apr), and declining until July, in the middle of the dry season[10]. High daytime and low night-time temperatures, associated with physiological costs of thermoregulation, have been shown to reduce survival and growth in pups[11], but, when allowing for potentially longer foraging time or higher success, may lead to an increase in the mass of adults[12].

When collecting trait and demographic data, not all individuals were weighed at each visit. Thus, to avoid bias due to missing mass measurements and measurement errors, we estimated the monthly body mass of each individual using the collected measurements. For pregnant females, we first discarded body mass measurements taken between 50 days before and 10 days after the end of pregnancy. For each month of age, we then fit generalized linear mixed models to body mass data with age-in-days and age-in-days^2 as the fixed effects and individual as random effect on both the mean and slope of age-in-days.

Using these models, we predicted the mass at each month of age for each individual. We used these individual monthly mass estimates for the rest of the analyses (see[1] for details). All mass measurements were transformed using the natural logarithm, following[13].

S1.2 Drivers of demographic rates and clinical TB

Rainfall and temperature deviations were not highly correlated (Pearson's correlation coefficient = - 0.35), and we therefore considered both in demographic-rate models.

Although they display dominant behaviour and are thus characterized as dominant in the IBM, natal dominant males essentially behave as helper males as they are very likely to emigrate from the group with other helpers. Thus, their demographic rates are modelled as helper rates (i.e., within the same model as male helpers).

When fitting demographic-rate models, we excluded (a) individual data where mass of an individual at the beginning of a given month could not be determined (usually because an individual had not yet been habituated to weighting; < 1% of data); or (b) data on group sizes where the latter could not be determined - this occurred in ca. 1 % of the recordings during very early stages of group formation in cases where individuals had to habituated.

We modelled individual survival and changes in mass (growth) using a binomial and normal distribution, respectively. Both the average and the variation in growth were assessed separately as functions of covariates. That is, growth variation was assumed to be heteroscedastic. We modelled emigration, immigration, and stage transitions using binomial distributions. Lastly, we modelled pup recruitment as a Poisson distribution (we tested and found no overdispersion in recruitment). The mass distribution of pups was modelled using a normal distribution. As with growth, the average and variation in pup mass were modelled as

functions of covariates, including the mass of the mother when the pups were still dependent (i.e., one month prior).

We tested for additive and two-way interaction effects of an individual's mass (or mother's mass when assessing pup mass), group size, season, temperature and rainfall deviation, and TB status (affected or not by clinical TB) of a group. For adult female survival and emigration rates, we also included pregnancy category (not pregnant, 1 month or 2 months pregnant, with pups) as a covariate. We also tested for the effect of age on female helper emigration (age as continuous covariate) and pup and juvenile (three categorical age classes) and subadult (six categorical age classes) survival and growth. For the probability of pregnancy, we further included the number of non-related males (i.e., immigrants) in the group as covariate. For male helper emigration, we also considered the ratio of females to males > 12 months of age as a covariate. In addition to a random year effect, we also tested for a random group-identity effect on demographic rates.

In parameterizing the GAMs, we used tensor product smooth terms (*te*), with thin-plate regression splines as the marginal bases for the effects of all continuous covariates with the exception of season and year. To model the effects of season (month-of-year), we used a cyclic cubic regression spline as the marginal basis to mimic seasonal cyclic patterns; to model year and group-identity effects, we used parametric terms (*s*) penalized by a ridge penalty as base. When applying smooths, we used three-knot locations for each covariate, with the exception of month, where we used four-knot location, following[13]. We also applied a degrees-of-freedom inflation factor (*gamma*) of 1.4 to all models to avoid overfitting due to overly flexible smooths. We used the *R* package *mgcv* to fit GAMs[14] and the package *MuMIn*[15] for model selection. Table S1.1 summarizes the most parsimonious models (see also S1.3 for plots of model predictions).

We note that GAMs for variation in growth and pup mass performed consistently poorly (explained < 5 % of variation in the residuals of the growth models). We therefore assumed constant variance.

Table S1.1 Most parsimonious GAM models for stage-specific demographic rates. * mass of the mother; Ma – mass; Y – year; Mo – month; Gs – group size; R – rainfall deviation; T – temperature deviation; A – age (months); PC – pregnancy category; NP – not pregnant: P1 – first-month pregnant; P2 – second-month pregnant; L – with weaning litter; IM - number of non-related immigrant males; R_{FM} - ratio of females to males. Functions $te(x_{df})$ and $s(x_{df})$ are the tensor product and spline smoothing functions of x, respectively, with the given degrees of freedom df. The df represents the amount of nonlinearity in the model component, where df=1 indicates linear fit. n is the corresponding sample size.

Life-cycle stage	Vital rate modeled	Link function	Best model	n
Pups	*Survival*	logit	$4.2_{(0.3)} - 1.5_{(0.3)}A_2 - 2.2_{(0.4)}A_3 + s(Y_{df:6.8}) + te(Ma, A_{1\ df:1.1}) + te(Ma, A_{2\ df:1.0}) + te(Ma, A_{3\ df:1.0}) + te(Gs, R_{df:4.3}) + te(Gs, T_{df:2..4}) + te(R, Mo_{df:2.5}) + te(T, Mo_{df:4.6})$	6372
	Growth (mass next)	identity	$5.8_{(0.0)} - 0.2_{(0.0)}A_2 - 0.3_{(0.0)}A_3 - 0.01_{(0.0)}TB_{yes} + s(Y_{df:20.4}) + te(Gs, A_{1\ df:1.8}) + te(Gs, A_{2\ df:0.8}) + te(Gs, A_{3\ df:0.8}) + te(Gs, Mo, TB_{no\ df:5.2}) + te(Gs, Mo, TB_{yes\ df:6.9}) + te(Ma, A_{1\ df:0.8}) + te(Ma, A_{2\ df:0.8}) + te(Ma, A_{3\ df:0.8}) + te(Ma, Gs_{df:3.9}) + te(Ma, Mo, _{df:1.8}) + te(Ma, R_{df:2.1}) + te(Ma, T_{df:5.7}) + te(R, Mo_{df:4.8}) + te(R, T_{df:2.0}) + te(T, Mo_{df:3.6}) + te(Ma, TB_{no\ df:0.7}) + te(Ma, TB_{yes\ df:3.3}) + te(R\ TB_{no\ df:4.8}) + te(R, TB_{yes\ df:4.8})$	5971
Juveniles	*Survival*	logit	$4.8_{(0.2)} - 0.5_{(0.2)}A_5 - 1.0_{(0.3)}A_6 + 0.1_{(0.4)}TB_{yes} + s(Y_{df:2.4}) + te(Gs, Mo_{df:1.0}) + te(Ma, Gs, TB_{no\ df:2.1}) + te(Ma, Gs, TB_{yes\ df:3.0}) + te(Ma, R_{df:4.8}) + te(Ma, T_{df:2.9}) + te(R, T_{df:1.0}) + te(T, Mo_{df:0.7})$	5606
	Growth (mass next)	identity	$6.1_{(0.0)} - 0.02_{(0.0)}A_5 - 0.04_{(0.0)}A_6 - 0.01_{(0.0)}TB_{yes} + s(Y_{df:20.6}) + te(Ma, Mo, TB_{no\ df:6.4}) + te(Ma, Mo, TB_{yes\ df:4.2}) + te(Ma, A_{4\ df:1.0}) + te(Ma, A_{5\ df:0.9}) + te(Ma, A_{6\ df:0.9}) + te(Ma, Gs_{df:1.7}) + te(Gs, Mo_{df:6.4}) + te(Gs, R_{df:5.3}) + te(Gs, T_{df:2.7}) + te(Ma, R_{df:1.6}) + te(Ma, T, _{df:5.0}) + te(R, Mo_{df:4.0}) + te(R, T_{df:1.9}) + te(T, Mo_{df:3.9}) + te(T, TB_{no\ df:1.1}) + te(T, TB_{yes\ df:1.9}) + te(R, TB_{no\ df:1.0}) + te(R, TB_{yes\ df:1.0})$	5475
Subadults	*Survival*	logit	$4.8_{(0.2)} + 0.2_{(0.3)}A_8 + 0.3_{(0.4)}A_9 - 0.4_{(0.3)}A_{10} - 0.9_{(0.3)}A_{11} - 1.2_{(0.3)}A_{12} - 0.8_{(0.2)}TB_{yes} + s(Y_{df:9.3}) + te(Gs, A_{7\ df:1.0}) + te(Gs, A_{8\ df:1.0}) + te(Gs, A_{9\ df:1.0}) + te(Gs, A_{10\ df:1.8}) + te(Gs, A_{11\ df:1.0}) + te(Gs, A_{12\ df:1.0}) + te(Gs, Mo_{df:0.8}) + te(Ma, Gs_{df:1.0}) + te(Ma, Mo_{df:0.9}) + te(R, Mo_{df:2.1}) + te(R, T, TB_{no\ df:3.0}) + te(R, T, TB_{yes\ df:4.7}) + te(Ma, TB_{no\ df:1.2}) + te(Ma, TB_{yes\ df:1.0}) + te(Ma, TB_{no\ df:1.2}) + te(Ma, TB_{yes\ df:0.0})$	9884
	Growth (mass next)	identity	$6.3_{0.1)} - 0.01_{(0.0)}A_8 - 0.02_{(0.0)}A_9 - 0.01_{(0.0)}A_{10} - 0.02_{(0.0)}A_{11} - 0.02_{(0.0)}A_{12} - 0.01_{(0.0)}TB_{yes} + s(Y_{df:20.5}) + te(Gs, A_{7\ df:1.8}) + te(Gs, A_{8\ df:1.7}) + te(Gs, A_{9\ df:0.9}) + te(Gs, A_{10\ df:1.3}) + te(Gs, A_{11\ df:0.9}) + te(Gs, A_{12\ df:0.9}) + te(Gs, Mo_{df:3.7}) + te(Gs, R_{df:1.5}) + te(Gs, T_{df:4.4}) + te(Ma, A_{7\ df:1.7}) + te(Ma, A_{8\ df:0.9}) + te(Ma, A_{9\ df:0.9}) + te(Ma, A_{10\ df:1.6}) + te(Ma, A_{11\ df:1.3}) + te(Ma, A_{12\ df:0.9}) + te(Ma, Gs_{df:3.0}) + te(Ma, Mo, TB_{no\ df:6.0}) + te(Ma, Mo, TB_{yes\ df:7.3}) + te(Ma, R_{df:2.8}) + te(Ma, T_{df:2.0}) + te(R, Mo_{df:4.0})$	9647

Table S1.1 continued

			+ *te*(R, T $_{df:0.7}$) + *te*(T, Mo $_{df:4.0}$) + *te*(Gs, TB$_{no\ df:0.8}$) + *te*(Gs, TB$_{yes\ df:0.8}$) + *te*(T, TB$_{no\ df:1.8}$) + *te*(T, TB$_{yes\ df:1.1}$) + *te*(R, TB$_{no\ df:1.0}$) + *te*(R, TB$_{yes\ df:1.0}$)	
Male helpers & natal dominants	*Survival*	logit	$4.0_{(0.1)} - 1.2_{(0.1)}TB_{yes}$ + *s*(Y $_{df:11.7}$) + *te*(Gs, Mo, TB$_{no\ df:1.0}$) + *te*(Gs, Mo, TB$_{yes\ df:4.7}$) + *te*(Gs, R $_{df:1.0}$) + *te*(Gs, T $_{df:1.6}$) + *te*(Ma, Gs $_{df:1.4}$) + *te*(Ma, Mo $_{df:3.2}$) + *te*(Ma, R $_{df:0.0}$) + *te*(Ma, T $_{df:0.0}$) + *te*(T, Mo $_{df:2.4}$) + *te*(R, TB$_{no\ df:1.4}$) + *te*(R, TB$_{yes\ df:1.6}$)	12943
	Emigration	logit	$-4.5_{(0.2)} - 0.9_{(0.3)}TB_{yes}$ + *s*(Y $_{df:18.2}$) + *te*(Gs, M, TB$_{no\ df:6.6}$) + *te*(Gs, M, TB$_{yes\ df:2.6}$) + *te*(Gs, R $_{df:7.8}$) + *te*(Ma, Gs $_{df:1.0}$) + *te*(Ma, T $_{df:4.9}$) + *te*(R, Mo $_{df:4.1}$) + *te*(R, T $_{df:3.3}$) + *te*(T, Mo $_{df:3.6}$)	12535
	Growth (mass next)	identity	$6.5_{(0.0)} - 0.0_{(0.0)}TB_{yes}$ + *s*(Y $_{df:18.5}$) + *te*(Gs, Mo, TB$_{no\ df:4.2}$) + *te*(Gs, Mo, TB$_{yes\ df:7.5}$) + *te*(Ma, Gs $_{df:4.2}$) + *te*(Gs, R $_{df:6.7}$) + *te*(Ma, Mo $_{df:5.1}$) + *te*(Ma, T $_{df:4.0}$) + *te*(Ma, R $_{df:2.0}$) + *te*(R, Mo $_{df:3.9}$) + *te*(R, T $_{df:5.8}$) + *te*(T, Mo $_{df:3.5}$) + *te*(Ma, TB$_{no\ df:0.8}$) + *te*(Ma, TB$_{yes\ df:1.4}$)	12332
Male helpers	*Immigration*	logit	$-3.7_{(0.2)} + 0.5_{(0.3)}TB_{yes}$ + *s*(Y $_{df:9.5}$) + *te*(Gs, Mo $_{df:4.6}$) + *te*(R$_{FM}$, Gs, TB$_{no\ df:3.0}$) + *te*(R$_{FM}$, Gs, TB$_{yes\ df:2.0}$) + *te*(R$_{FM}$, Mo $_{df:1.0}$) + *te*(T, Mo $_{df:3.9}$)	3254
	# immigrant	log	$0.6_{(0.1)}$ + *te*(Mo $_{df:1.0}$)	149
Immigrant dominant males	*Survival*	logit	$8.4_{(1.5)} - 5.4_{(1.5)}TB_{yes}$ + *te*(Gs, Mo $_{df:1.0}$) + *te*(Gs, T, TB$_{no\ df:3.9}$) + *te*(Gs, T, TB$_{yes\ df:3.0}$) + *te*(Ma, Mo $_{df:4.0}$) + *te*(Ma, R $_{df:3.0}$) + *te*(Ma, T $_{df:2.6}$) + *te*(R, Mo $_{df:2.3}$)	1270
	Emigration	logit	$-9.8_{(2.2)} + 2.4_{(2.4)}TB_{yes}$ + *te*(Gs, Mo $_{df:1.7}$) + *te*(Ma, Gs, TB$_{no\ df:3.0}$) + *te*(Ma, Gs, TB$_{yes\ df:2.0}$)	1243
	Growth (mass next)	identity	$6.6_{(0.2)} - 0.0_{(0.0)}TB_{yes}$ + *s*(Y $_{df:15.5}$) + *te*(Gs, Mo $_{df:2.7}$) + *te*(Ma, Mo $_{df:5.1}$) + *te*(R, Mo, TB$_{no\ df:3.9}$) + *te*(R, Mo, TB$_{yes\ df:3.4}$) + *te*(T, Mo $_{df:2.7}$) + *te*(Ma, TB$_{no\ df:1.0}$) + *te*(Ma, TB$_{yes\ df:1.7}$)	1240
Female helpers	*Survival*	logit	$4.6_{(0.1)} - 1.5_{(0.2)}TB_{yes}$ + *te*(Gs, Mo $_{df:1.0}$) + *te*(Gs, T $_{df:3.7}$) + *te*(Ma, Mo, TB$_{no\ df:2.2}$) + *te*(Ma, Mo, TB$_{yes\ df:1.9}$) + *te*(R, Mo $_{df:2.5}$)	8219
	Emigration	logit	$-4.5_{(0.2)} + 0.2_{(0.3)}PC_{P2}$ + $0.9_{(0.2)}$PC$_{NP}$ – $0.6_{(0.3)}$TB$_{yes}$ + *s*(Y $_{df:13.1}$) + *te*(Gs, Mo $_{df:6.1}$) + *te*(Gs, R $_{df:4.6}$) + *te*(Ma, Mo $_{df:1.8}$) + *te*(Ma, T $_{df:3.0}$) + *te*(R, Mo $_{df:0.9}$) + *te*(T, Mo, TB$_{no\ df:5.6}$) + *te*(T, Mo, TB$_{yes\ df:6.5}$) + *te*(A, Ma $_{df:2.1}$) + *te*(R, TB$_{no\ df:1.0}$) + *te*(R, TB$_{yes\ df:1.0}$)	9410
	Growth (mass next)	identity	$6.9_{(0.1)}$ - $0.01_{(0.0)}$PC$_{P2}$ - $0.0_{(0.0)}$PC$_{L}$ + $0.01_{(0.0)}$PC$_{NP}$ – $0.01_{(0.0)}$TB$_{yes}$ + *s*(Y $_{df:18.8}$) + *te*(Gs, PC$_{P1\ df:0.8}$) + *te*(Gs, PC$_{P2\ df:0.8}$) + *te*(Gs, PC$_{L\ df:0.8}$) + *te*(Gs, PC$_{NP\ df:1.6}$) + *te*(Ma, PC$_{P1\ df:1.3}$) + *te*(Ma, PC$_{P2\ df:0.8}$) + *te*(Ma, PC$_{L\ df:0.8}$) + *te*(Ma, PC$_{NP\ df:0.8}$) + *te*(Gs, Mo, TB$_{no\ df:1.9}$) + *te*(Gs, Mo, TB$_{yes\ df:7.3}$) + *te*(Gs, T $_{df:3.4}$) + *te*(Ma, Gs $_{df:2.5}$) + *te*(Ma, Mo $_{df:6.2}$) + *te*(Ma, T $_{df:3.9}$) + *te*(R, Mo $_{df:5.7}$) + *te*(R, T $_{df:3.0}$) + *te*(T, Mo $_{df:2.5}$)	9259
	Transition NP to P1	logit	$-2.8_{(0.1)}$ - $0.1_{(0.1)}$TB$_{yes}$ + *s*(Y $_{df:16.1}$) + *te*(Gs, R, TB$_{no\ df:3.0}$) + *te*(Gs, R, TB$_{yes\ df:2.4}$) + *te*(Gs, T $_{df:7.4}$) + *te*(Ma, Mo $_{df:0.0}$) + *te*(R, Mo $_{df:5.0}$) + *te*(T, Mo $_{df:2.2}$) + *te*(IM, Gs $_{df:2.1}$) + *te*(Ma, TB$_{no\ df:1.0}$) + *te*(Ma, TB$_{yes\ df:1.0}$)	7819

Table S1.1 continued

	Transition P1 to P2 or abort	logit	$1.5_{(0.1)} - 0.4_{(0.2)}TB_{yes}$ + *te*(Gs, T $_{df:3.6}$) + *te*(R, Mo, $TB_{no\ df:2.9}$) + *te*(R, Mo, $TB_{yes\ df:2.3}$)+ *te*(T, Mo, $_{df:0.0}$)	772
	Transition P1 to P1 if abort	logit	$-2.6_{(0.3)}$ + *s*(Y $_{df:0.7}$) + *te*(Ma $_{df:1.0}$)	155
	Transition P2 to L or abort	logit	$-0.9_{(0.1)} + 0.05_{(0.2)}TB_{yes}$ + *te*(Gs, Mo $_{df:3.8}$) + *te*(Gs, R, $TB_{no\ df:3.0}$) + *te*(Gs, R, $TB_{yes\ df:2.0}$) + *te*(Ma, Mo $_{df:0.8}$) + *te*(R, Mo $_{df:0.7}$)	588
	Transition P2 to P1 if abort	logit	$-2.9_{(0.3)}$ + *te*(Ma, Gs $_{df:3.0}$) + *te*(R $_{df:1.7}$)	408
	Transition L to P1 or NP	logit	$-2.5_{(1.7)} - 2.7_{(2.3)}TB_{yes}$ + *te*(Gs $_{df:1.5}$) + *te*(Ma $_{df:1.0}$) + *te*(T $_{df:1.0}$) + *te*(Mo, $TB_{no\ df:1.8}$) + *te*(Mo, $TB_{yes\ df:1.6}$)	206
	# recruits	log	$1.0_{(0.1)}$ + *te*(Ma $_{df:1.0}$) + *te*(Gs $_{df:1.0}$)	201
	Offsping mass	identity	$4.8_{(0.0)} - 0.1_{(0.0)}TB_{yes}$ + *s*(Y $_{df:18.5}$) + *te*(Gs, Mo $_{df:7.0}$) + *te*(Gs, R $_{df:4.9}$) + *te*(Ma*, Gs $_{df:3.1}$) + *te*(Ma*, Mo $_{df:2.1}$) + *te*(Ma*, R $_{df:5.9}$) + *te*(Ma*, T $_{df:2.4}$) + *te*(R, Mo, $TB_{no\ df:7.5}$) + *te*(R, Mo, $TB_{yes\ df:2.8}$) + *te*(R, T $_{df:3.9}$) + *te*(T, Mo $_{df:1.9}$) + *te*(T, $TB_{no\ df:1.7}$) + *te*(T, $TB_{yes\ df:0.8}$)	472
Dominant females	*Survival*	logit	$5.1_{(0.4)} - 0.8_{(0.4)}PC_{NP} - 1.2_{(0.3)}TB_{yes}$ + *s*(Y $_{df:2.6}$) + *te*(Gs, Mo $_{df:1.0}$) + *te*(Gs, T $_{df:2.1}$) + *te*(Ma, Gs $_{df:1.1}$) + *te*(Ma, Mo $_{df:0.8}$) + *te*(T, Mo $_{df:0.8}$)	1651
	Growth (mass next)	identity	$6.6_{(0.0)} - 0.01_{(0.0)}PC_{P2} - 0.0_{(0.0)}PC_{L} + 0.00_{(0.0)}PC_{NP} - 0.01_{(0.0)}TB_{yes}$ + *s*(Y $_{df:13.4}$) + *te*(Gs, Mo $_{df:0.6}$) + *te*(Ma, $PC_{P1\ df:1.0}$) + *te*(Ma, $PC_{P2\ df:1.4}$) + *te*(Ma, $PC_{L\ df:1.0}$) + *te*(Ma, $PC_{NP\ df:1.0}$) + *te*(T, Gs, $TB_{no\ df:2.3}$) + *te*(T, Gs, $TB_{yes\ df:4.1}$) + *te*(Ma, Gs $_{df:2.8}$) + *te*(R, Mo $_{df:2.7}$) + *te*(R, T $_{df:4.2}$) + *te*(T, Mo $_{df:3.8}$)	2521
	Transition NP to P1	logit	$-0.6_{(0.1)} - 0.3_{(0.2)}TB_{yes}$ + *s*(Y $_{df:1.5}$) + *te*(Gs, Mo, $TB_{no\ df:1.5}$) + *te*(Gs, Mo, $TB_{yes\ df:6.5}$) + *te*(Gs, R $_{df:3.0}$) + *te*(Gs, T $_{df:1.8}$) + *te*(Ma, Mo $_{df:3.6}$) + *te*(Ma, R $_{df:0.0}$) + *te*(R, Mo $_{df:3.9}$) + *te*(R, T $_{df:0.9}$) + *te*(T, Mo $_{df:3.1}$) + *te*(IM, Mo $_{df:2.7}$)	1006
	Transition P1 to P2 or abort	logit	$2.3_{(0.2)} - 0.5_{(0.3)}TB_{yes}$ + *s*(Y $_{df:0.5}$) + *te*(Ma, Gs $_{df:5.0}$) + *te*(Ma, Mo $_{df:5.1}$) + *te*(Ma, R $_{df:1.0}$) + *te*(Ma, T $_{df:1.0}$) + *te*(R, T $_{df:3.0}$) + *te*(T, Mo $_{df:0.0}$)	579
	Transition P1 to P1 if abort	logit	$-2.5_{(0.9)}$ + *te*(Gs $_{df:1.0}$) + *te*(R $_{df:1.8}$)	81
	Transition P2 to L or abort	logit	$1.1_{(0.1)} - 0.7_{(0.2)}TB_{yes}$ + *te*(Gs, Mo $_{df:1.0}$) + *te*(Ma, Mo $_{df:2.2}$) + *te*(Ma, T $_{df:3.6}$) + *te*(R, Mo $_{df:0.0}$) + *te*(R, T $_{df:1.0}$) + *te*(T, Mo $_{df:1.0}$)	592

Table S1.1 continued

Transition P2 to P1 if abort	logit	$-1.4_{(0.2)}$ + *te*(Ma $_{df:1.0}$) + *te*(R, T $_{df:3.1}$)	176
Transition L to P1/P2 or abort	logit	$0.4_{(0.1)} - 0.9_{(0.3)}TB_{yes}$ + *s*(Y $_{df:6.1}$) + *te*(Gs, Mo, $TB_{no\ df:4.9}$) + *te*(Gs, Mo, $TB_{yes\ df:1.3}$) + *te*(Ma, Mo $_{df:1.0}$) + *te*(Ma, R $_{df:1.0}$) + *te*(Ma, T $_{df:1.0}$) + *te*(T, Mo $_{df:3.2}$)	441
Transition L to P2 if not aborted	logit	*Constant* (p = 0.32)	249
# recruits	log	$1.3_{(0.0)} - 0.1_{(0.07)}TB_{yes}$ + *te*(Gs, Mo $_{df:1.6}$) + *te*(Ma, Gs $_{df:1.0}$) + *te*(Ma, Mo $_{df:0.8}$)	446
Offsping mass	identity	$4.8_{(0.0)}$ - $0.05_{(0.01)}TB_{yes}$ + *s*(Y $_{df:17.1}$) + *te*(Gs, Mo $_{df:4.3}$) + *te*(Gs, T $_{df:1.3}$) + *te*(Ma*, Gs, $TB_{no\ df:6.9}$) + *te*(Ma*, Gs, $TB_{yes\ df:3.6}$) + *te*(Ma*, Mo $_{df1.6}$) + *te*(Ma*, T $_{df:231}$) + *te*(R, Mo $_{df:5.6}$) + *te*(R, T $_{df:5.1}$) + *te*(T, Mo $_{df:3.2}$)	1488

S1.3 Demographic rate predictions

Detailed plots of meerkat demographic-rate predictions are shown as supporting data figure (*vitalRatesPred.pdf*) on Zenodo (see page 1 of SM). Predictions were obtained from the most parsimonious generalized additive models. For each demographic rate, different subplots show average predictions (lines) ± 95 % prediction interval (shaded area) for different combinations of predictors. Predictors not shown on subplots were held constant. In the plots, TB = at least one individual in the groups has clinical TB; and no TB = no individuals in the group show clinical TB.

Details

As has been shown in the previous studies[1,13,16,17], here too all demographic rates increase with mass, or the mothers' mass in the case of pup mass. Survival, growth, and reproduction are generally highest at intermediate group sizes and decrease in small or very larger groups and are higher in relatively cooler (negative temperature deviations from seasonal means) and wetter (positive rainfall deviations) months. However, the effects of climate variation on these demographic rates strongly depend on season. The effect of individual,

social, and environmental factors on survival and growth of males does not differ substantially from the effects on females. Immigration of male helpers into the group decreases with group size but increases with the ratio of females to males in a group.

Overall, clinical TB in the group affects demographic rates of subadults and adults more than those of pups and juveniles. After clinical TB appears in adult individuals in a given group, survival of adults decreases, particularly when group size is small. Decreases in mass when a group shows clinical TB also occur, but mainly in dominant males; for the remaining life-cycle stages, mass becomes more variable in clinical-TB affected groups. Both male and female helper emigration is generally lower in clinical-TB affected groups than unaffected ones. Emigration of dominant males is slightly higher in clinical-TB affected groups. Immigration decreases substantially with group size after a group has clinical TB cases, while this decrease is slower when a group has no cases.

For adults, survival is lowest after clinical TB cases are observed in the group (Fig. S1.3) and group size is small, particularly under thermal stress (high temperature deviations). Growth of female and male helpers, meanwhile, varies substantially more across seasons (months) and climatic conditions when a group has clinical TB than when it has no clinical TB cases. Emigration of males and females is highest in small groups under high rainfall and temperature deviation. The probability of reproducing (transitioning from NP to P1) is higher for female helpers when the group has clinical TB cases, but only under above-average rainfall. However, the chances of female helpers carrying a pregnancy to term (transitioning from P1 to P2 and then to L) or immediately becoming pregnant (transitioning to P1) after aborting or losing a litter are substantially reduced and vary more among seasons and climates in a group with clinical TB cases; these chances are also generally lowest in large groups. If a pregnancy is successfully carried to terms, female helpers have more but lighter pups after clinical TB is observed in the group.

Similar to female helpers, dominant females have lowest survival after clinical TB is observed in their group and the group is small and under thermal stress (high temperature deviations). The survival, growth, and reproduction of dominant females also vary more across environmental conditions when individuals in their group have clinical TB. Carrying a pregnancy to term and pup numbers are reduced in dominant females after a group has developed clinical TB (see Table S1.1). The chances of immediate pregnancy after aborting are higher in a clinical-TB affected group, especially under abundant rainfall.

Comparison to observed data

GAM predictions fit well with observed patterns of demographic-rate variation. Below (Fig. S1.1-S1.7), we show average monthly predicted and observed values for demographic rates. Note that the we show monthly averages taken from individual mean predictions. Prediction intervals are shown in *vitalRatesPred.pdf*. We note that for binomial vital rates for which observed mean monthly values are close to or at 0 or 1, averages from predictions are more variable. This is in due to the robust GAM modelling that provided smoothed predictions to avoid parameter overfitting to extreme values. At the same time, we sample discrete (0,1) values from the GAM predictions in the IBM, and this results in simulated numbers of adults, group sizes, and masses being within the range of observed values (Supporting Material S3) – and providing the best approximations of observed patterns in meerkats thus far[13].

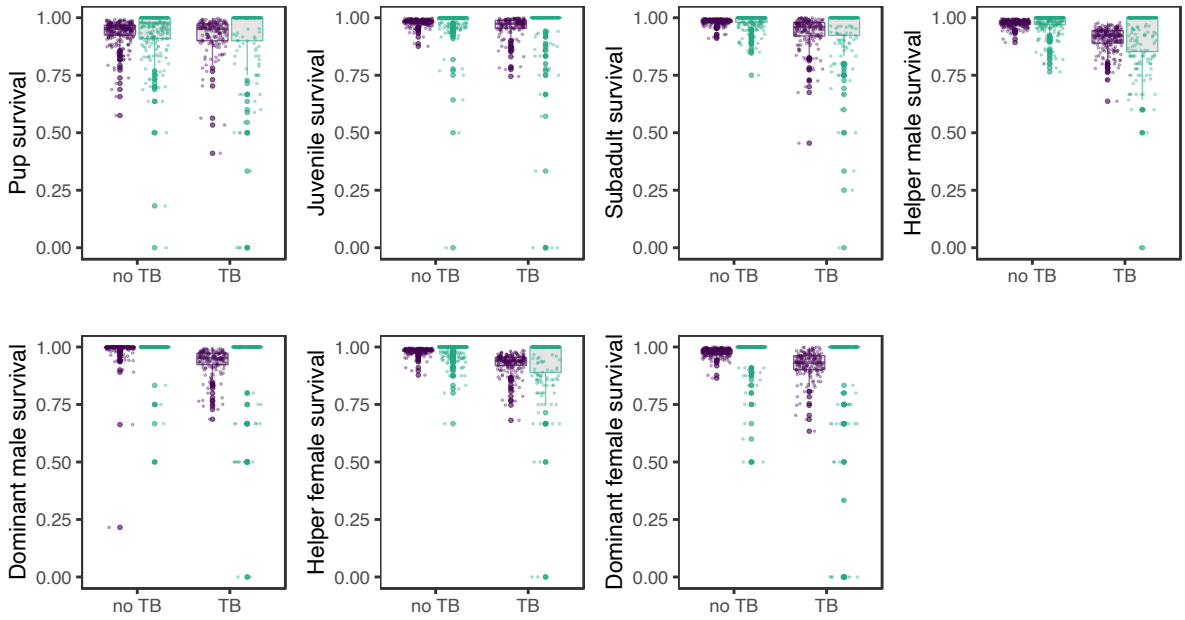

Figure S1.1 Predicted (purple) vs. observed (blue-green) stage-specific meerkat survival rates. Points show monthly averages (over individuals and groups) of observed and mean predicted (from most parsimonious GAMs in Table S1.1) survival rates. Boxplots summarize the distribution of the average monthly survival rates. Rates are divided between occasions where no clinical TB (no TB) was detected in groups or at least one group member showed clinical TB.

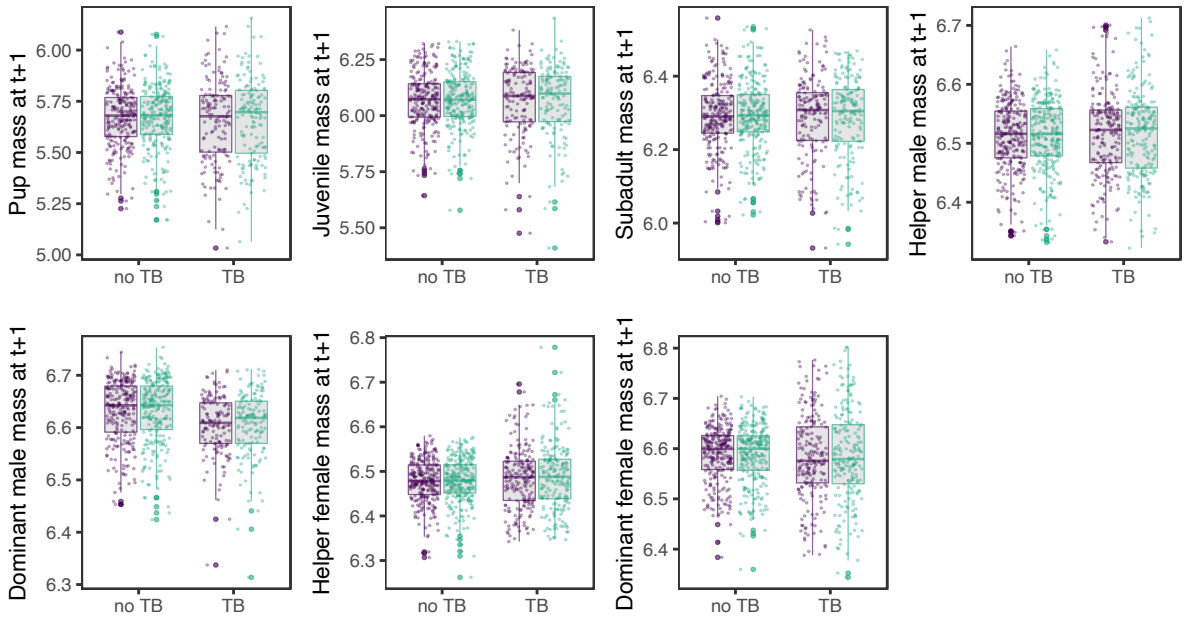

Figure S1.2 Predicted (purple) vs. observed (blue-green) stage-specific meerkat mass change. Points show monthly averages (over individuals and groups) of observed and mean predicted (from most parsimonious GAMs in Table S1.1) masses (log grams). Boxplots summarize the distribution of the average monthly masses. Mass averages are divided between occasions where no clinical TB (no TB) was detected in groups or at least one group member showed clinical TB.

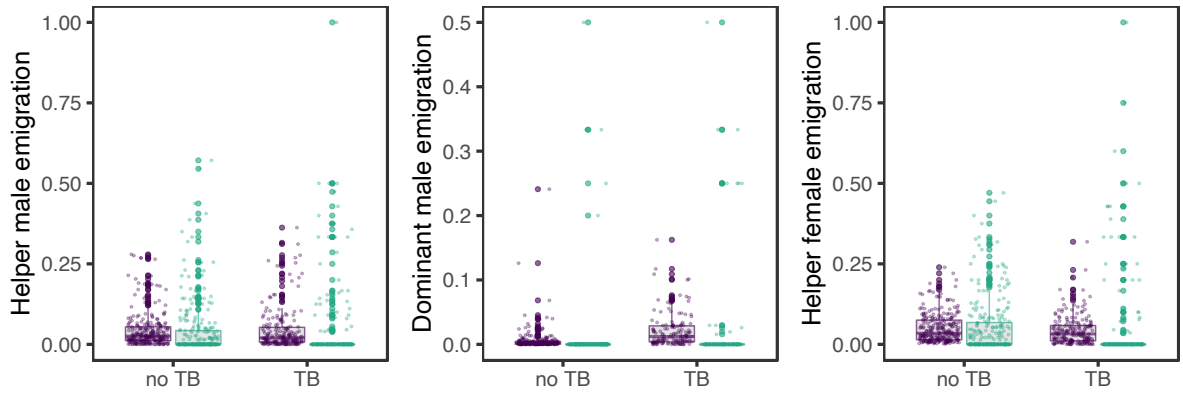

Figure S1.3 Predicted (purple) vs. observed (blue-green) stage-specific meerkat emigration rates. Points show monthly averages (over individuals and groups) of observed and mean predicted (from most parsimonious GAMs in Table S1.1) emigration rates. Boxplots summarize the distribution of the average monthly emigration rates. Rates are divided between occasions where no clinical TB (no TB) was detected in groups or at least one group member showed clinical TB.

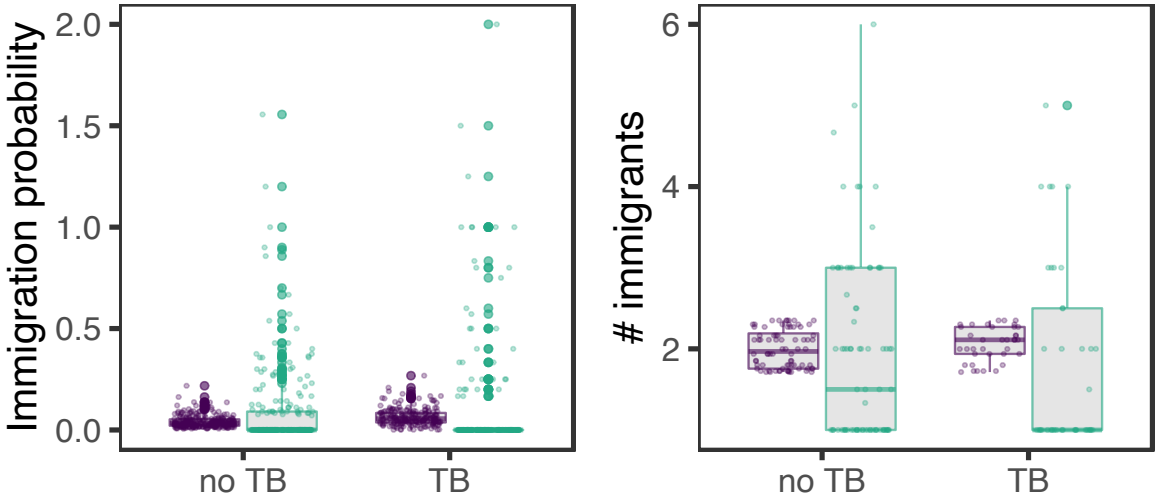

Figure S1.4 Predicted (purple) vs. observed (blue-green) stage-specific meerkat immigration rates and numbers. Points show monthly averages (over groups) of observed and mean predicted (from most parsimonious GAMs in Table S1.1) immigration patterns. Boxplots summarize the distribution of the average monthly values. Rates are divided between occasions where no clinical TB (no TB) was detected in groups or at least one group member showed clinical TB.

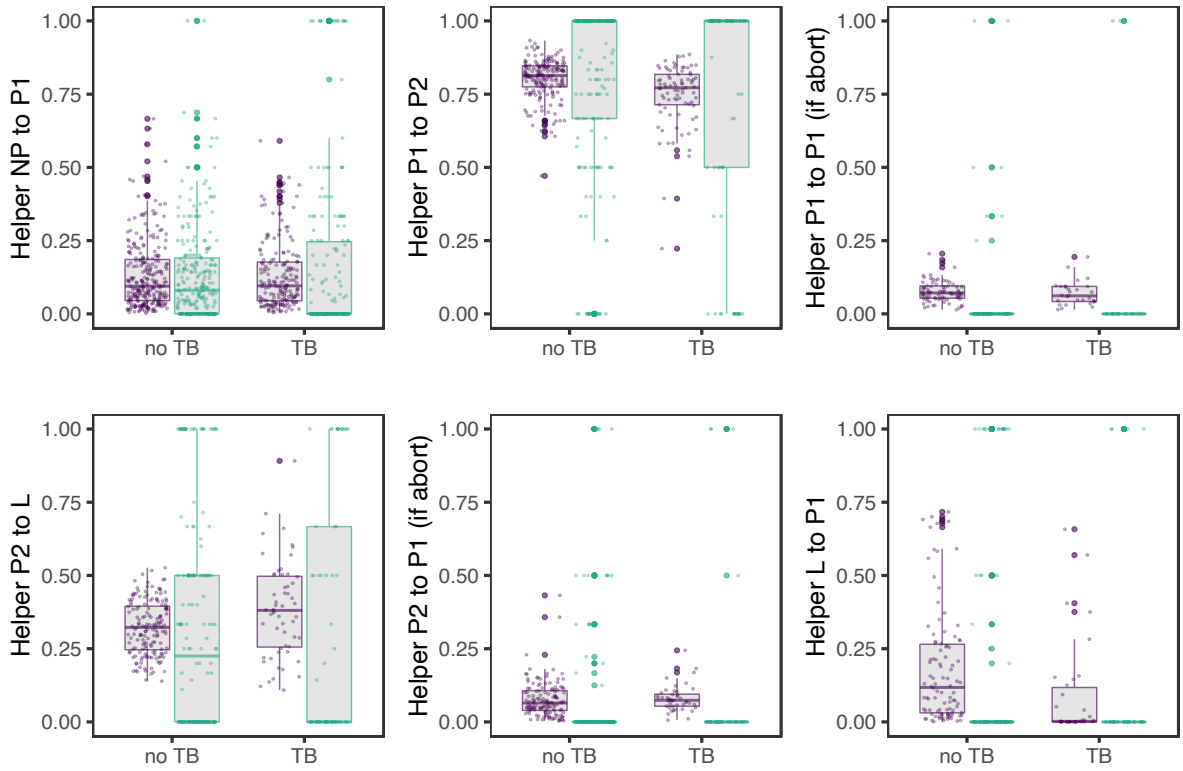

Figure S1.5 Predicted (purple) vs. observed (blue-green) transitions among pregnancy states in female helpers. Points show monthly averages (over individuals and groups) of observed and mean predicted (from most parsimonious GAMs in Table S1.1) transitions. Boxplots summarize the distribution of the average monthly transition rates. Rates are divided between occasions where no clinical TB (no TB) was detected in groups or at least one group member showed clinical TB. NP – not pregnant: P1 – first-month pregnant; P2 – second-month pregnant; L – with weaning litter.

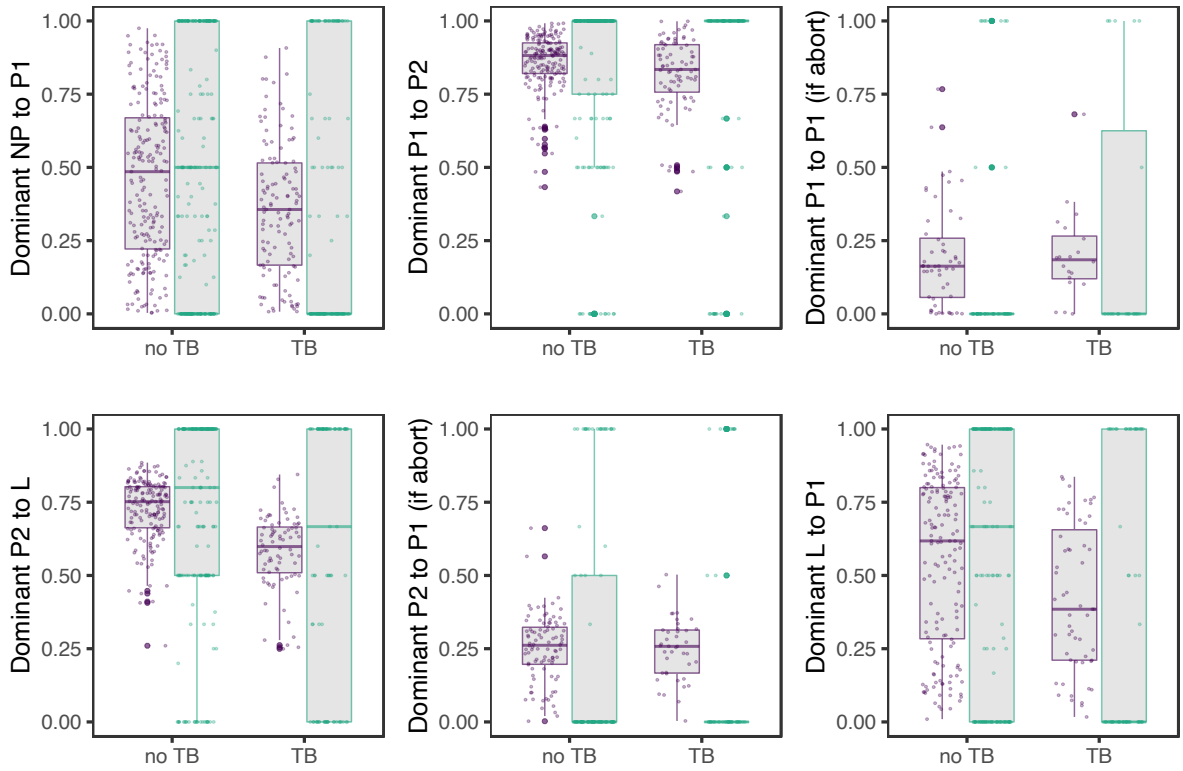

Figure S1.6 Predicted (purple) vs. observed (blue-green) transitions among pregnancy states in dominant females. Points show monthly averages (over individuals and groups) of observed and mean predicted (from most parsimonious GAMs in Table S1.1) transitions. Boxplots summarize the distribution of the average monthly transition rates. Rates are divided between occasions where no clinical TB (no TB) was detected in groups or at least one group member showed clinical TB. NP – not pregnant: P1 – first-month pregnant; P2 – second-month pregnant; L – with weaning litter.

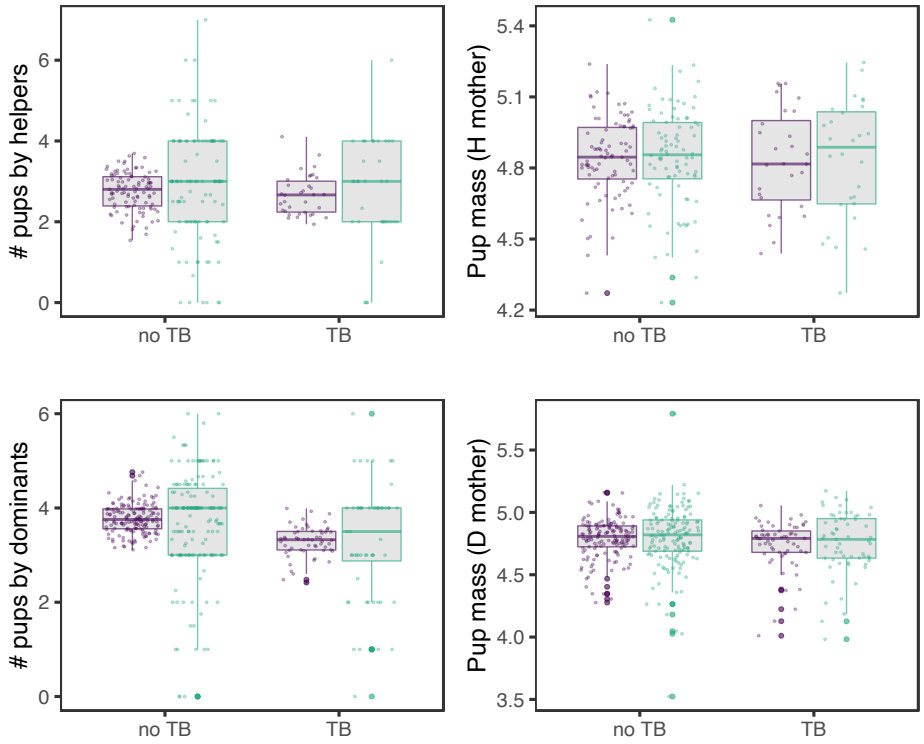

Figure S1.7 Predicted (purple) vs. observed (blue-green) recruitment and pup mass. Points show monthly averages (over individuals and groups) of observed and mean predicted (from most parsimonious GAMs in Table S1.1) values. Boxplots summarize the distribution of the average monthly pup numbers and pup masses. Results are divided between occasions where no clinical TB (no TB) was detected in groups or at least one group member showed clinical TB. H – helper; D – dominant

The effects of dispersal on temperature-TB dynamics we discuss in the main text are also supported by the empirical data.

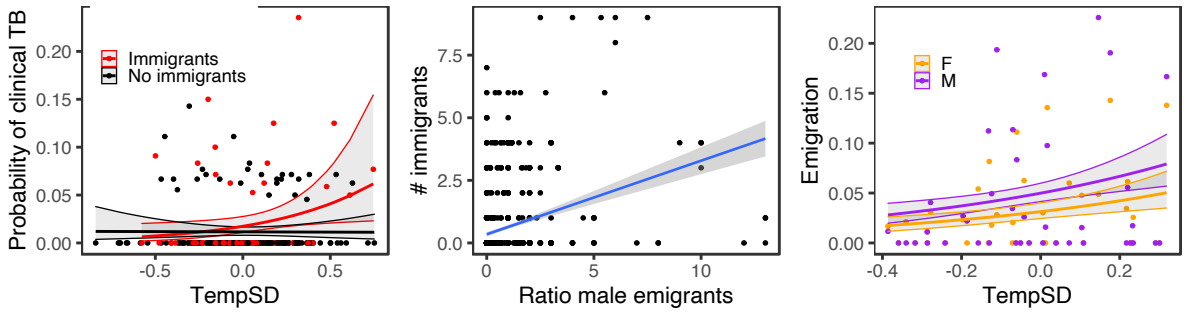

Figure S1.8 Observed relationships between climate, TB outbreaks, and migration. Points show observed average monthly values, while lines show predictions (± 95 % prediction interval as shaded areas) from simple generalized (clinical TB and female [F] and male [M] emigration probabilities) or linear (# of immigrants) models. Immigrants/no immigrants depicts whether immigration has occurred in the five months prior to first TB signs. Ratio of male to female emigrants is shown in the centre plot.

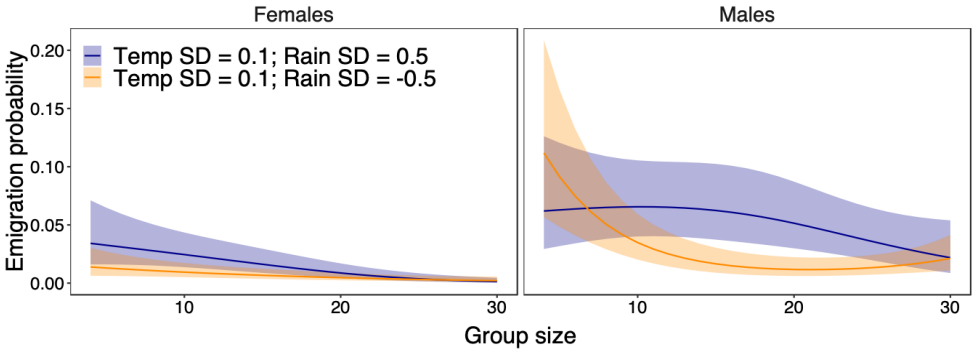

Figure S1.9 Complementary plot to Figure 3c in main text. Plots show predictions (± 95 % prediction interval as shaded area) of GAM models for stage-specific emigration. Predictions were obtained by setting constant other predictors in the models, either to their averages or to month = 6 for seasonal effects, which correspond to the months with the highest numbers of immigrants. Probabilities prior to the occurrence of first clinical TB cases are shown. Group size refers to the number of subadults (7-12 months old) and adults (> 12 months old) in a group. The weather effects are plotted as positive or negative deviations (SD) of maximum temperatures and rainfall from their seasonal means.

S1.4 Probability of clinical, end-stage TB

We used a GAM parameterization analogous to demographic-rate models to assess drivers of the first clinal signs of TB (> 0 individuals show lumps). Groups were particularly likely to show clinical TB when temperature was higher than the seasonal average (temperature SD > 0) and groups had received a relatively high number of male immigrants in the five months prior to first clinical TB.

Table S1.2 Most parsimonious GAM model for the probability of at least one individual in a group having clinical TB. tempSD – temperature deviation; IM - number of immigrant males. Function $te(x_{df})$ are the tensor product smoothing functions of x, with the given degrees of freedom df. The df represents the amount of nonlinearity in the model component, where df=1 indicates linear fit. n is the corresponding sample size.

Entity modelled	Link function	Best model	n
First occurrence of clinical TB	logit	$-4.4_{(0.2)} + te(\text{tempSD, IM}_{\text{df:3.0}})$	1788

Supporting Material S2 – IBM protocol

We note that all data and code to visualize past climate trends (`Kalahari_climate_past.R`), build the IBM and project it under baseline

(`meerkat_group_IBM_baseline.R`), and scenarios of increases in extreme temperatures (`meerkat_group_IBM_scen_extreme.R`); as well as to assess the risk of extremes under climate change (`meerkat_gcm_risks.R`) are freely available.

Overview, Design concepts, Details (ODD) protocol

The description of the individual-based model (IBM) simulating meerkat group dynamics (ED Fig. 3) follows the ODD (Overview, Design concepts, Details) protocol commonly used for describing individual- and agent-based models[18]. Below, the first three sections provide the model overview, the fourth section explains general concepts underlying the model design, and the remaining sections provide further model and analysis details.

1. Purpose

The purpose of our model is to investigate the effect of individual, social and environmental factors on group dynamics of a group-living mammal under climate change. The model is designed to simulate individual fates and traits (body mass) via demographic-rate models, while considering climatic (rainfall and temperature deviations from seasonal means) and group-level (group size, ratios of females to males, number of male immigrants, and clinical TB status) information when parameterizing these models. Specifically, we developed this model to investigate whether climate change threatens groups primarily via direct effects of rainfall and temperature on individual demographic rates or via indirect effects through disease outbreak.

2. Entities, state variables, and scales

The meerkat IBM is a single-species, two-sex, discrete-time population model with each time step representing one month. It comprises two hierarchical levels: individuals and social groups. All individuals in this analysis are characterized by the following state variables: individual identity, mother's identity, sex, age (in months), monthly mass (log of body mass in grams), natal group identity, social stage, and, where appropriate, immigration status (natal or immigrant males) and reproductive stage (pregnant, with litter, or non-reproductive

females). The social groups have the group identity and TB status (no clinical TB or at least one clinical TB case) as state variables. The 11 main social stages included in the model are as follows: pup (1-3 months of age); juvenile (4-6 months); subadult (7-12 months); male, and non-pregnant, pregnant, or weaning (with litter) subordinate female helper (>12 months); and male, and non-pregnant, pregnant, or weaning (with litter) female dominant (>12 months) (Fig. S1.1)[19].

The individual phenotypic trait used in our model is monthly body mass (i.e. the natural logarithm of body mass measured in grams). The model's environmental factors and their seasonal fluctuations are characterized by month-of-year and rainfall and temperature deviation from means taken over the previous 1.5 months (for details on calculations see [1,13]). Here, we assumed that the state variable, body mass, accounted for the cumulative environmental effects earlier than previous 1.5 months[20]. The model's social factors comprise the effective group size (number of individuals > 6 months of age), the number of immigrant adult (> 12 months of age) males, and the ratio of adult females-to-males. Lastly, clinical TB is modelled at the group level, and all individuals in a group get assigned the status clinical TB "yes" when after clinical signs of TB (swellings) have been observed in at least one individual[21]. Nevertheless, within a given group TB status (yes or no), demographic rates are modelled at the stage-specific and individual levels, and the effects of TB (which cannot be reliably observed for all individuals in a group) on different are indirectly captured. For instance, helper survival decreases more than dominant female survival under clinical TB compared to no apparent TB, as end-stage, clinical TB has been observed more frequently in adult helpers[21].

3. Process overview and scheduling

Our model simulates the fate and body mass of each individual within a social group from their birth (or beginning of simulations) to death (or end of simulations). Individuals transition among social stages following a set of demographic rates, i.e., survival, growth, emigration,

immigration, and reproduction (Table S1.1). The demographic rates of survival, emigration, immigration, reproduction, and recruitment determine the fate of individuals; while growth and recruit-mass functions determine changes in body mass (ED Fig. 3). Reproduction takes place over three months[6] and involves three stages: pregnancy over two months (P1 and P2), successful birth of litters (L) and recruitment (weaning of one-month old pups, R). The recruits are randomly assigned a sex, assuming a 1:1 sex ratio[22]. From one month to the next, individuals survive or die, and those that survive grow. Adults can emigrate or stay in a group, and those that stay can become dominant or stay subordinate (based on their age and mass). Male adults can also immigrate into a group as helpers or incumbent dominants. Because female immigration into established social groups has never been observed[23], we assume zero female immigration in our model. Female adults can get pregnant, and those that conceive either give birth successfully or lose the litter (before or at birth). Those that do give birth wean a certain number of month-old pups with a certain body mass. The functions determining each of these demographic rates are described in the '*Submodels*' section, and the links between different processes in the model are shown in diagrammatic form in ED Fig. 3. At each time step, each of the demographic rates is age- and stage-specific and differentially affected by body mass, number of helpers (in some cases also number of immigrants and female-male ratios), rainfall and temperature deviations, season (month-of-year), and group TB status.

The IBM simulates individuals within a group from one month to the next, and after all individuals complete the monthly processes, their age and social stage are updated simultaneously. At the beginning of each time step, the group size is estimated as the number of individuals older than six months, because meerkats start helping behaviour around six months of age[24]. If a group does not have clinical TB cases, we also determine its probability to become get at least one clinical TB case. A clinical TB-affected group cannot subsequently transition to a state without apparent TB cases. Simulations are carried out separately for each of 10 groups; they start at the observed initial conditions and run

sequentially from 2019 to 2059 or until the simulated group goes extinct. We chose the observed initial conditions to represent various group sizes and compositions (see Table S3.1 for details).

4. Design concepts

Basic principles. The key design concept of our model is the link between individual processes and group dynamics. The importance of such links, particularly when investigating global-change effects on natural populations, has been emphasized in recent theoretical and empirical studies, e.g., [25–27].

Emergence. In our model, group dynamics emerge as a result of individual fates, and individual fates are imposed stochastically from empirically observed relationships between stage-specific demographic processes. These, in turn, depend on individual traits and social and environmental factors. The demographic processes produce new trait values and group characteristics in a given month, which are then used as cumulative effects of past conditions to project dynamics of several social groups. Group dynamics emerge from these hierarchical, non-linear relationships.

Interactions. Individuals within a group interact indirectly through the effect of group size, number of immigrant males, and female/male ratios on demographic rates. Direct interactions occur during the re-assignment of dominance status (see *Individual-based model (IBM)* in the *Methods* section in the main text).

Stochasticity. Variation in demographic rates and probability of clinical TB that is not explained by individual, social, and environmental factors (and random year effect) is included as random noise. The IBM then includes stochasticity by using this variation to sample new values for demographic rates.

Collectives. The submodels describing each demographic rate are fit to data from each sex and main life-history or social stage separately; therefore, individuals in each stage are governed by the same functions of individual, environmental, and social parameters (though affected differently by stochastic noise).

Observations. At each time step of the simulations, we record the individual's identity, mother's identity, sex, age, mass, social stage, and, where appropriate immigration status (natal or immigrant males) and reproductive stage (pregnant, with litter, or non-reproductive females). We also record the clinical-TB status of the group and update rainfall and temperature values.

5. Initialization

The initial state of a given social group is the same for each simulation for that group and includes the identity, sex, age, mass, social stage, and, where appropriate, immigration status and reproductive stage of each individual that was present in the group at the start of the observations. At the start of observations, all 10 groups are free of clinical TB. The starting month and year for a given social group are set to 1 January 2019.

6. Input Data

Initial group compositions and climate data are the only external inputs that are not affected by the internal dynamics of the model.

7. Submodels

For parameterization of the demographic-rate submodels, we used the individual-level data of 1,194 females and 1,497 male meerkats from 85 groups to generate monthly, discrete-step censuses of individuals between January 15, 1997 and December 15, 2018. The demographic rates consisted of monthly survival (0 or 1), mass change, emigration (0 or 1), immigration (0 or 1), number of immigrants (≥1), transitions among pregnancy states (0 or

1), recruitment (number of pups weaned, ≥0), and pup mass (Table S1.1). As reproduction took place after the 12th month of life, reproduction, recruitment, and offspring mass were modelled only for the helper and dominant female stages (separately). As recruitment is the number of pups that leave the burrow around 20-30 days (i.e., detectable litter size), it also includes the survival of pups from birth to weaning. All recruits are randomly assigned a sex, assuming a 1:1 sex ratio, i.e., a probability of 0.5 to be either female or male.

8. Final output metrics and synthetic likelihood

We calculated synthetic likelihoods by comparing the simulated output metrics to observed data for the 10 groups. IBM simulations are used to obtain the mean and the covariance matrix of the statistics, given model parameters, and this then allow for the construction of a likelihood that assesses model fit. We used a subset of the output metrics: number of immigrants; average, and coefficient of variation in group size, numbers of adults, and stage-specific adult body mass; and a modified measure of reproductive success, i.e., average monthly numbers of pups. Extinction and clinical TB probabilities were excluded because they were calculated across simulation runs only. For the remaining excluded metrics, comparisons to observed data were not possible across all groups, as two of the starter groups went extinct less than one year after establishment. This created zero-inflation (e.g., in the number of migrants), small sample sizes (e.g., no CV in male numbers), no pups surviving until adulthood. However, we quantified the synthetic likelihood again for the five groups for which we could incorporate all metrics. Adding metrics did not change the likelihood patterns across different IBM implementations and further emphasizes that modelling clinical TB is more important for a good model fit to observed data than modelling climate (Fig. S2.1).

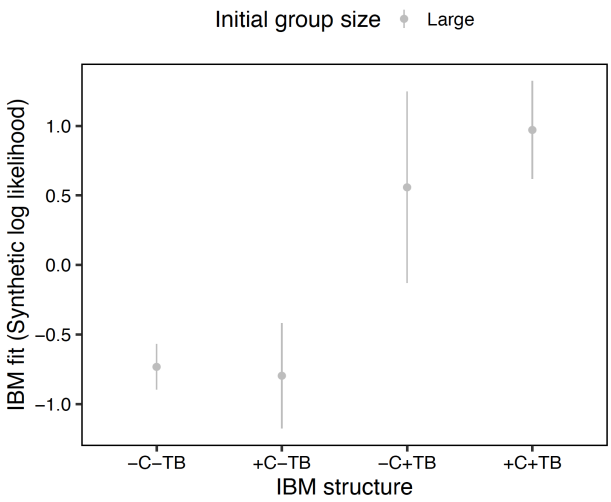

Figure S2.1. IBM performance improves for established groups when TB status and, to a lesser extent, climate deviations are considered in demographic-rate models. Synthetic log-likelihoods are based on comparing all 14 simulated summary statistics to observed data for groups that were observed for < 2 years. These groups also had relatively higher initial group sizes at the start of IBM simulations (groups 6-10 in Table S3.1). The points and bars represent mean and standard error of synthetic log likelihoods among the five groups. Climate deviations (C) and TB status were either included (+) or excluded (-) when parameterizing demographic rates used in the IBM.

Supporting Material S3 – IBM output

For the cooperatively breeding meerkats, group size is a key determinant of individual fitness and group persistence, and the composition of a group can play an important role in how groups interact with dispersing individuals and other groups. We therefore wanted to account for a range of group compositions when initialising IBM simulations and assess how these may affect our results. Table S3.1 summarises these initial conditions.

Table S3.1 Some initial characteristics of the 10 meerkat groups used for simulations. Groups differed in size, sex ratios, and stage distributions. Groups also differed in age composition and number of immigrant males (see *init.group.comp.csv*).

467

Group ID	# females	# males	stages	Starting date (for perturbations)
1	2	1	2 helper females; 1 subadult male	2004-12-15
5	3	2	4 helpers; 1 dominant (female)	2011-06-15
3	4	2	5 helpers; 1 dominant (male)	2006-08-15
4	1	1	helpers	2007-02-15
5	2	2	2 helpers; 1 dominant pair	2001-11-15
6	11	11	4 juveniles; 9 subadults; 7 helpers; 1 dominant pair	2001-01-15
7	6	10	4 pups; 2 juveniles; 8 helpers; 1 dominant pair	2008-04-15
8	10	8	4 pups; 2 juveniles; 4 subadults; 6 helpers; 1 dominant pair	1998-01-15
9	8	11	3 pups; 3 juveniles; 11 helpers; 1 dominant pair	2011-01-15
10	10	18	6 pups; 3 juveniles; 8 subadults; 10 helpers; 1 dominant female	2011-01-15

S3.1 IBM simulation fit to observed data

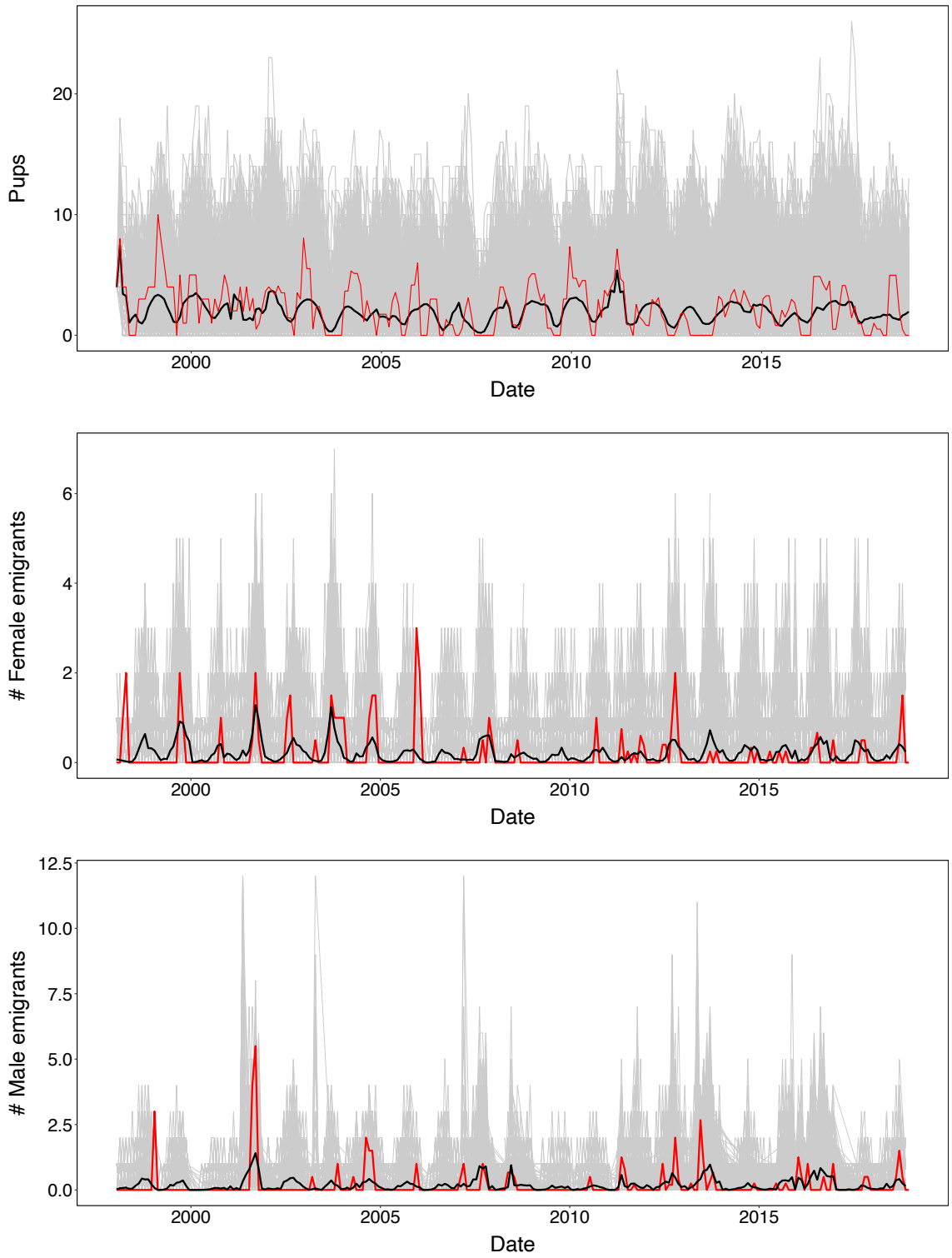

Figure S3.1. Simulated numbers of 1-month old pups and emigrants fall within the distribution of observed numbers. Simulations were based on the individual-based model which projected dynamics of 10 groups, including reproductive output, in discrete monthly intervals for the duration of the group's lifespan (or until Dec 2018). Red line: Average total observed number of pups and emigrants across the 10 groups. Black line: average simulated total number of pups/emigrants across

the 10 groups and 1000 simulation runs. Grey lines: average total number of pups/emigrants in each simulation run. Total number (n) of data points to calculate observed and simulated numbers is n = 251 and n = 256076, respectively.

Assessing the above-described complex interactions between demography, climate, and TB are important to accurately capture group dynamics in the IBM (i.e., improve its predictive power). However, this is only true when simulating fates of initially medium-sized to large groups, where including clinical TB infection primarily improves the output of the IBM, with a smaller contribution of climate (Fig. S3.2).

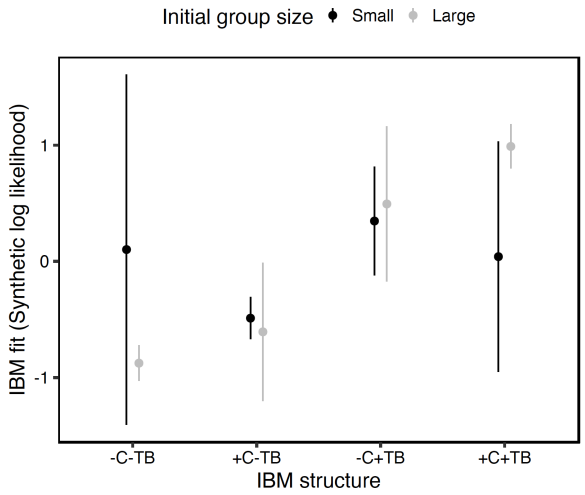

Figure S3.2. IBM performance improves when climate and TB status are considered in demographic-rate models and group extinction is not driven by stochastic mortality. Synthetic log-likelihoods are based on comparing nine simulated summary statistics to observed data (see Supporting Material S2 for details). The points and bars represent mean and standard error, respectively, of synthetic log likelihoods among five small and medium/large groups at the beginning of simulations. Climate (C; deviations of rainfall and temperatures from monthly means) and TB status were either included (+) or excluded (-) when parameterizing demographic rates used in the IBM.

S3.2 IBM simulations using future projected climate values

Climate data (1979-2020) show that although annual mean maximum temperatures (Fig. 1) as well as monthly mean maximum temperatures (Fig. S3.3) have been increasing, rainfall does not show clear trends, although variation in rainfall has increased slightly (Fig. S3.4). For maximum temperatures, increases were significant 1979-2012 (95% CI of slope from

linear fit of temperature as a function of time did not cross 0) and have accelerated from 2013 on at the annual scale (Fig. 1) and for months 9-12.

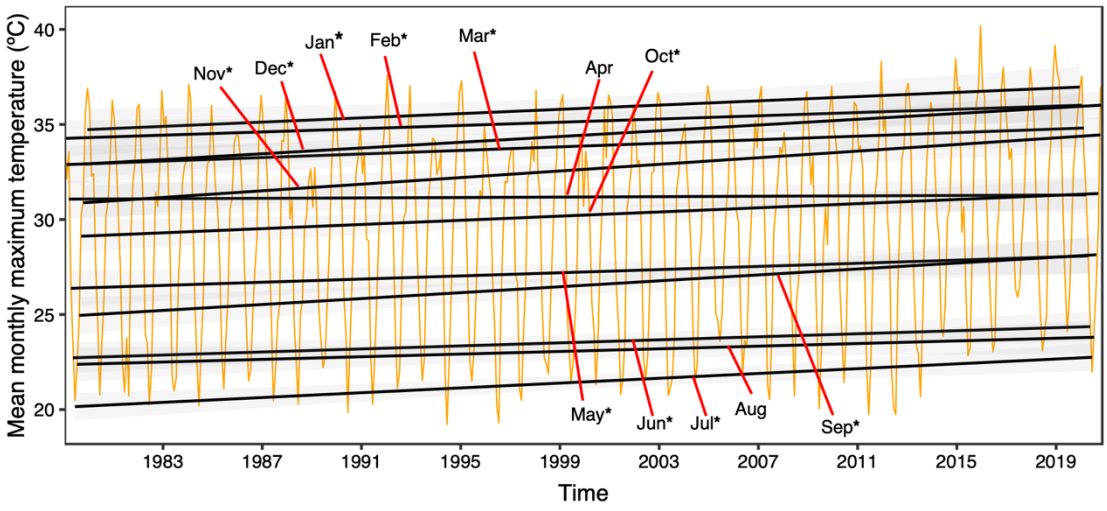

Figure S3.3. Monthly trends in maximum temperatures at the study site. Orange line depicts observed values, as interpolated by NOAA CPC, while black lines depict mean predictions (± 95 % prediction intervals as shaded areas) from simple linear models fit to temperature values through time for each month. Stars indicate significant slope coefficients of the models (95% CI did not cross 0).

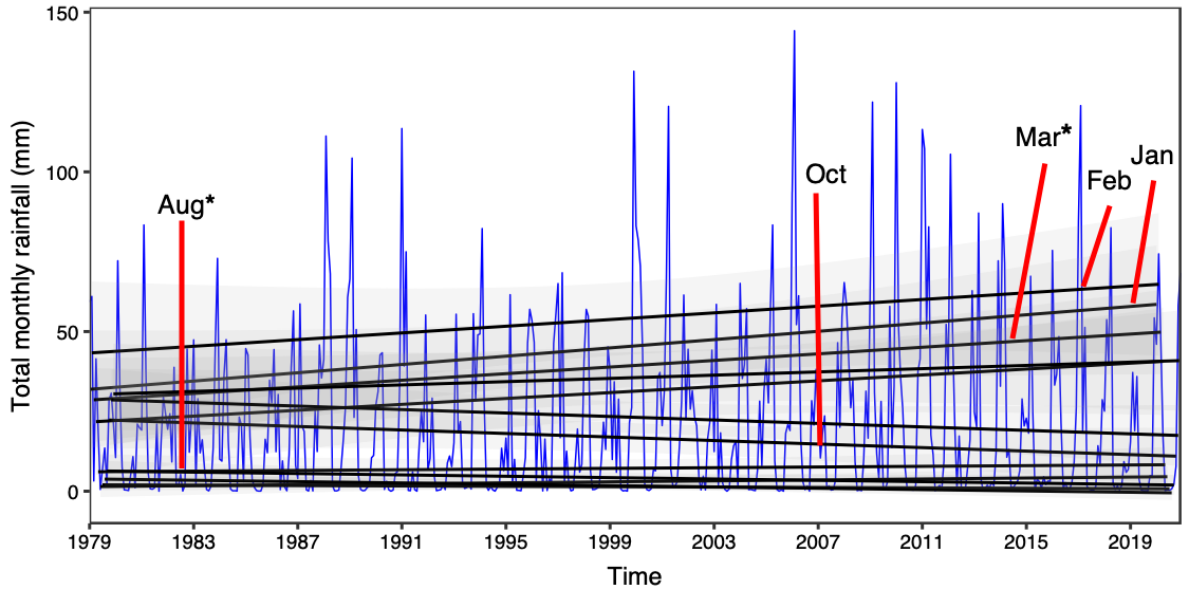

Figure S3.4. Monthly trends in total rainfall at the study site. Blue lines depict observed values, as interpolated by NOAA CPC, while black lines depict mean predictions (± 95 % prediction intervals as shaded areas) from simple linear models fit to rainfall values for each month. Stars indicate significant slope coefficients of the models (95% CI did not cross 0).

We therefore focused on testing sensitivities of meerkat group dynamics to increases in episodes of above-average maximum temperatures. To do so, we defined increasingly extreme *hot years*, i.e., years in which scaled maximum temperatures were above their long-

term (1997-2018) averages for > 6, > 7, > 8, >9, or > 10 months. This corresponded to years ’99, ’05, ’07, ’09, ’10, ’14-’18; years ’05,’10, ’14-’18; years ’10, ’14-’18; years ’10, ’15, ’16, ‘18; and years ’15 and ’16, respectively. In all those years, above-average temperatures occurred in at least one month in the pre-breeding season (July- September); in the years ’05, ´15, ’16, and ‘18, maximum temperatures were above the 90th percentile of their distribution for two months. In addition, years of increases in temperature extremes did not correspond to years in rainfall extremes. Projecting group dynamics assuming the probability of sampling these years to be 0.6 or 0.9 and comparing these projections to a baseline (no *hot years*) showed that group extinction probabilities increased for all scenarios, but were particularly sensitive (steepest increase) to increases in the extreme years 2015 and 2016 (ED Fig. 6).

We next quantified climate-impact risks by assessing changes in temperature extremes as defined by our scenarios under climate-change models from the Coupled Model Intercomparison Project 5 (CMIP5). We downloaded historical simulations (1997-2005) and projections (2006-2100) of mean monthly maximum temperatures from 21 global change models (GCMs) (https://esgf-node.llnl.gov/projects/cmip5/). To work with the greatest variation of GCM outputs, we chose models that differed most in their underlying code and parameterisation of underlying conditions[28]. Most of the GCMs have been used in other ecological studies[29]. We also ensured that historical estimates (1997-2005) and simulations of current conditions (2006-2018) did not produce unrealistic values of maximum temperatures for the Kalahari.

Table S3.2. CMIP5 General Circulation Models from which climate projections were used in this study. This table can also be found here: https://pcmdi.llnl.gov/mips/cmip5/availability.html

Modeling Center	Model	Institution	terms of use
BCC	BCC-CSM1.1(m)	Beijing Climate Center, China Meteorological Administration	unrestricted
CCCma	CanESM2	Canadian Centre for Climate Modelling and Analysis	unrestricted
CNRM-CERFACS	CNRM-CM5	Centre National de Recherches Meteorologiques / Centre Europeen de Recherche et Formation Avancees en Calcul Scientifique	unrestricted
CSIRO-BOM	ACCESS1.0	CSIRO (Commonwealth Scientific and Industrial Research Organisation, Australia), and BOM (Bureau of Meteorology, Australia)	unrestricted
CSIRO-QCCCE	CSIRO-Mk3.6.0	Commonwealth Scientific and Industrial Research Organisation in collaboration with the Queensland Climate Change Centre of Excellence	unrestricted
EC-EARTH	EC-EARTH	EC-EARTH consortium	unrestricted
FIO	FIO-ESM	The First Institute of Oceanography, SOA, China	unrestricted
GCESS	BNU-ESM	College of Global Change and Earth System Science, Beijing Normal University	unrestricted
INM	INM-CM4	Institute for Numerical Mathematics	unrestricted
IPSL	IPSL-CM5A-LR IPSL-CM5A-MR	Institut Pierre-Simon Laplace	unrestricted
LASG-CESS	FGOALS-g2	LASG, Institute of Atmospheric Physics, Chinese Academy of Sciences; and CESS, Tsinghua University	unrestricted
MIROC	MIROC5	Atmosphere and Ocean Research Institute (The University of Tokyo), National Institute for Environmental Studies, and Japan Agency for Marine-Earth Science and Technology	unrestricted
MIROC	MIROC-ESM-CHEM	Japan Agency for Marine-Earth Science and Technology, Atmosphere and Ocean Research Institute (The University of Tokyo), and National Institute for Environmental Studies	unrestricted
MPI-M	MPI-ESM-MR	Max Planck Institute for Meteorology (MPI-M)	unrestricted
MRI	MRI-CGCM3	Meteorological Research Institute	unrestricted
NASA GISS	GISS-E2-H GISS-E2-R	NASA Goddard Institute for Space Studies	unrestricted
NCAR	CCSM4	National Center for Atmospheric Research	unrestricted
NCC	NorESM1-M	Norwegian Climate Centre	unrestricted
NOAA GFDL	GFDL-ESM2G	Geophysical Fluid Dynamics Laboratory	unrestricted

For each GCM we downloaded up to four future scenarios of atmospheric greenhouse gas Representative Concentration Pathways (RCPs) depicting the level of radiative forcing (i.e., enhanced greenhouse effect) by the year 2100 (note that for some GCMs, RCP2.6 or RCP6.0 were not available; *gcm_output.csv*). RCPs include one high pathway where radiative forcing reaches 8.5 Watts per square meter (Wm^{-2}) by 2100 (RCP 8.5), two intermediate pathways in which radiative forcing is stabilized at 4.5 Wm^{-2} and 6.0 Wm^{-2} after 2100 (RCP 4.5 and RCP 6.0), and one low pathways in which radiative forcing peaks around 3 Wm^{-2} before 2100 and then declines (RCP 2.6). We calculated standardized deviation of maximum temperatures from their current monthly means (1997-2018) for the entire time series. We used temperatures interpolated at the grid point closest to the study site, but using averages of the four closest grid points did not change our results.

Using the GCM projections, we finally calculated the proportion of models that indicate that hot years (i.e., >6, 7, 8, 9, or >10 months if above-average temperatures) will at least double by mid century (2041-2061) and by end century (2079-2100) for each RCP.

Figure S3.5 shows the importance of accounting for TB dynamics when projecting climate-change effects on meerkat groups.

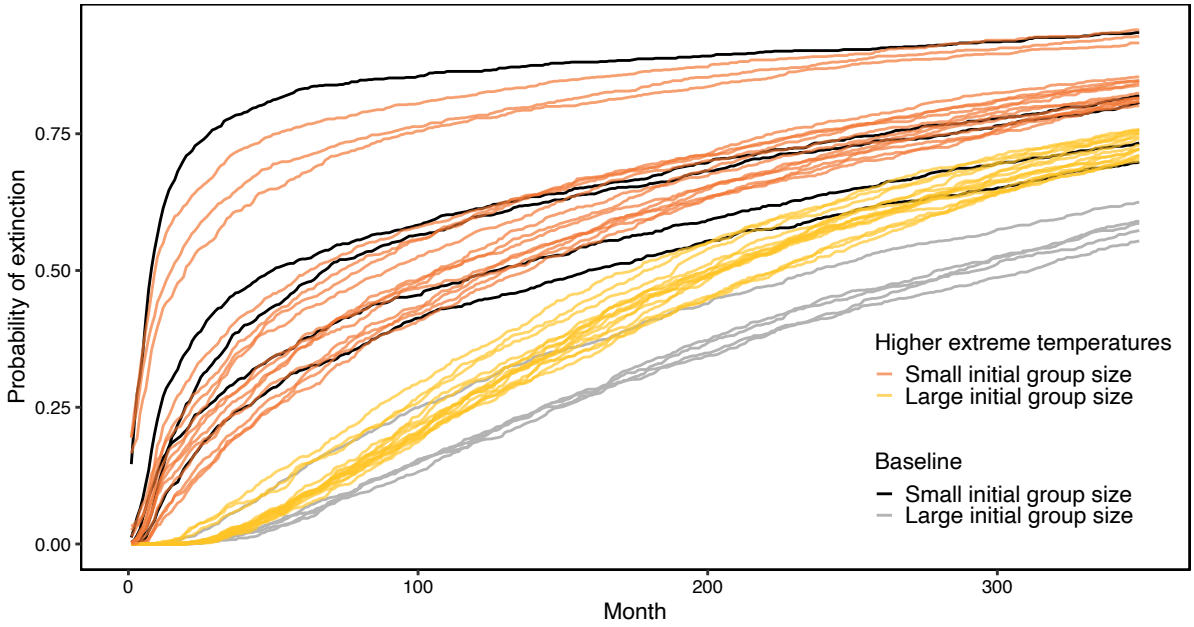

Fig. S3.5. Projections of meerkat group dynamics under climate change excluding TB dynamics in underlying models. Lines show cumulative probabilities of extinction by a given date (month), calculated as the proportion of 1000 IBM simulations in which groups go extinct. Different lines show different groups that vary in their initial conditions (< 7 and > 10 individuals in initially small and large group, respectively) at the start of simulations under baseline simulations (projecting values of rainfall and temperature deviation observed 1997-2012) and under climate change simulations (projecting values observed 2013-2018).

S3.3 Output metrics from IBM projections

We visually inspected changes in all IBM output metrics under different climate-TB perturbations that were incorporated into all demographic rate predictions simultaneously. We focused on full factorial perturbations where no extremes (no extreme years) or projected future extremes of temperature and rainfall deviations were sampled (sampling extremely hot years, 2015 and 2016, with a probability of 0.75), and the probabilities of clinical TB varied or was set to 0 in simulations

Below, Figures S3.8-S3.16 show key metrics describing group dynamics under IBM projections. The projections consisted of full factorial design where past (PC; sampling

temperature and rainfall 1997-2014, 2017, 2018) or future climate trends (FC; sampling temperature and rainfall 2015 & 2016 with probability of 0.75) were projected, and the probabilities of clinical TB in a group varied (+TB) or was set to 0 in simulations (-TB). The figures depict results for groups that were small or medium/large-sized when simulations started (see Table S3.1); and across simulations that resulted in group persistence or extinction after 12 years.

In general, compared to scenarios where neither climate change nor TB affect groups (PC-TB), the effects on group metrics of omitting clinical TB under climate change (FC-TB) are stronger than omitting climate change while allowing for clinical TB (PC+TB), suggesting that disease is central in increasing rates of group extinction.

In simulations where groups go extinct, group sizes, and number of adults are smaller, and the number of immigrant males is much higher, than in groups that persist throughout the projections. In the latter case, the strongest effect generally occurs when allowing for TB and climate change (FC+TB) and when the groups are initially medium/large; and setting clinical TB probability to 0 (FC-TB) under climate change does not dramatically improve metrics compared to simulation where past climate is maintained, either in combination with clinical TB (PC+TB) are omitting the latter (PC-TB). This suggests that climate effects, more than TB, are driving group dynamics in larger persisting groups. In groups that go extinct, preventing clinical TB improves averages in group metrics and decreases variance across simulations substantially (e.g., numbers of adults are largest and their variance lowest under PC-TB and FC-TB; and the opposite is true under PC+TB and FC+TB); and this is particularly true for small initial group sizes. This strongly suggest that climate-change impacts on group persistence operate largely via clinical TB and group size and destabilize group dynamics.

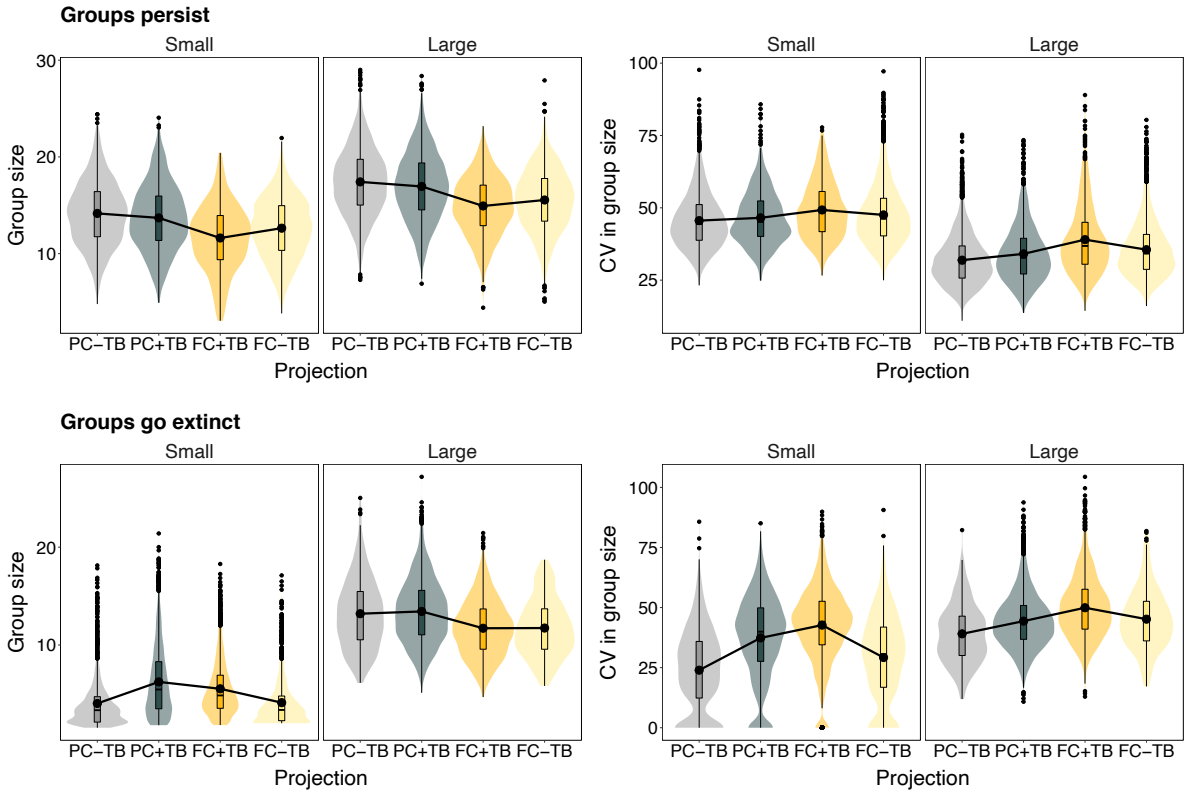

Figure S3.6. Effects of climate and clinical TB on mean and CV of group size. Boxplots and violin plots show the distribution of average number of individuals > 6-months old as well as CV in this number, for initially small and medium/large groups, across projections of the IBM where extinction did not occur vs. where it occurred after 12 years. Projections are based on four scenarios: allowing for TB (+TB) or keeping probability of clinical TB = 0 (-TB) while using observed past climate deviations (PC) in demographic models or sampling assumed future values (FC).

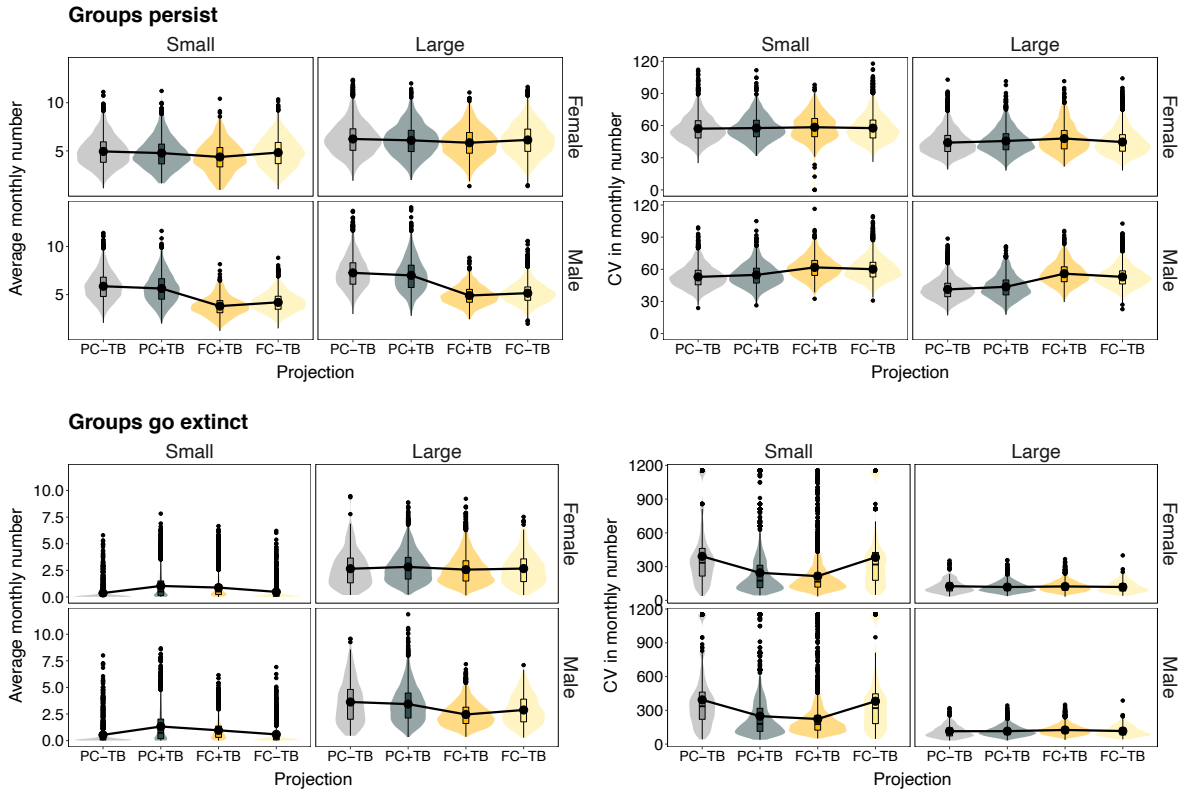

Figure S3.7. Effects of climate and clinical TB on mean and CV of adult numbers in a group. Boxplots and violin plots show the distribution of average number of adult meerkats (> 12 months old) as well as CV in this number, for initially small and medium/large groups, across projections of the IBM where extinction did not occur vs. where it occurred after 12 years. Projections are based on four scenarios: allowing for TB (+TB) or keeping probability of clinical TB = 0 (-TB) while using observed past climate deviations (PC) in demographic models or sampling assumed future values (FC).

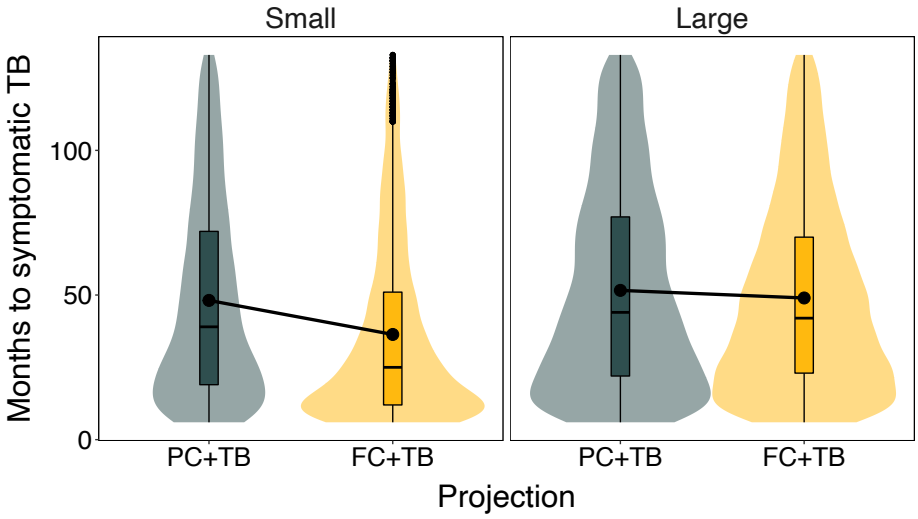

Figure S3.8. Effects of climate and TB perturbations on time to clinical TB cases occurring in a group. Boxplots and violin plots show the distribution of months to TB for initially small and medium/large groups, across projections of the IBM where extinction did not occur vs. where it occurred after 12 years. Projections are based on two scenarios: allowing for TB (+TB) and using observed past climate deviations (PC) in demographic models or sampling assumed future values (FC).

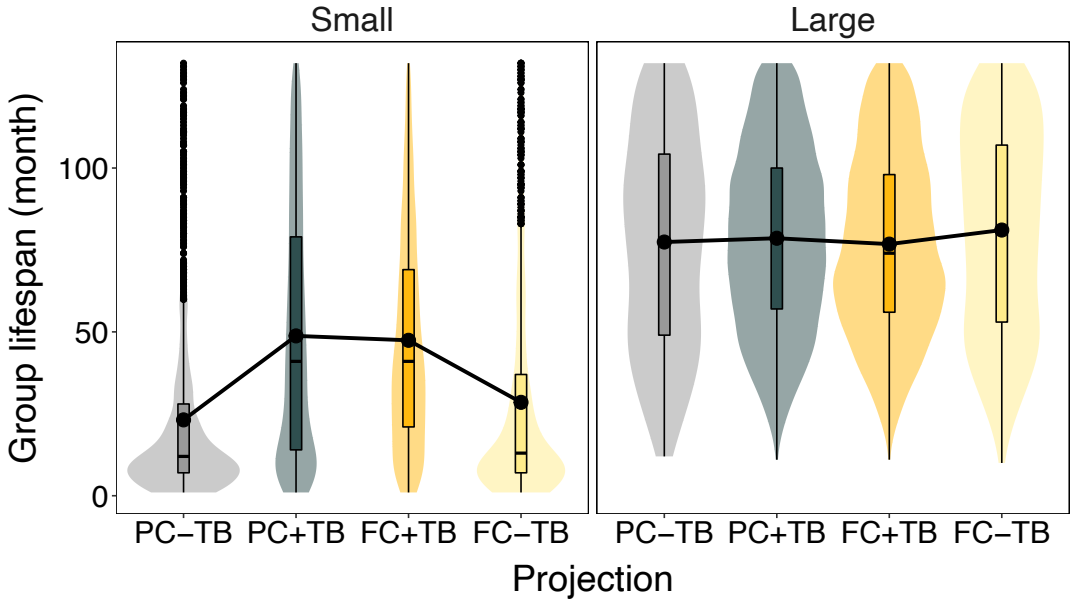

Figure S3.9. Effects of climate and clinical TB on lifespan (group age in months at extinction). Boxplots and violin plots show the distribution of lifespans, for initially small and medium/large groups, across projections of the IBM where extinction did not occur vs. where it occurred after 12 years. Projections are based on four scenarios: allowing for TB (+TB) or keeping probability of clinical TB = 0 (-TB) while using observed past climate deviations (PC) in demographic models or sampling assumed future values (FC).

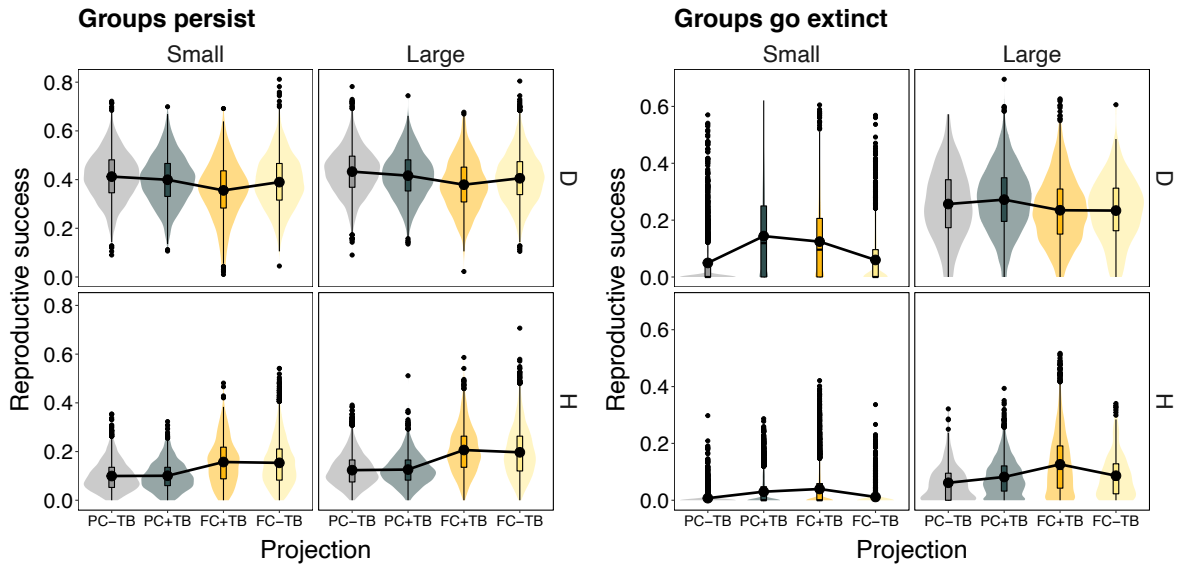

Figure S3.10. Effects of climate and clinical TB on reproductive success (monthly average number of pups surviving to > 12 months) for female dominants (D) and helpers (H). Boxplots and violin plots show the distribution for initially small and medium/large groups, across projections of the IBM where extinction did not occur vs. where it occurred after 12 years. Projections are based on four scenarios: allowing for TB (+TB) or keeping probability of clinical TB = 0 (-TB) while using observed past climate deviations (PC) in demographic models or sampling assumed future values (FC).

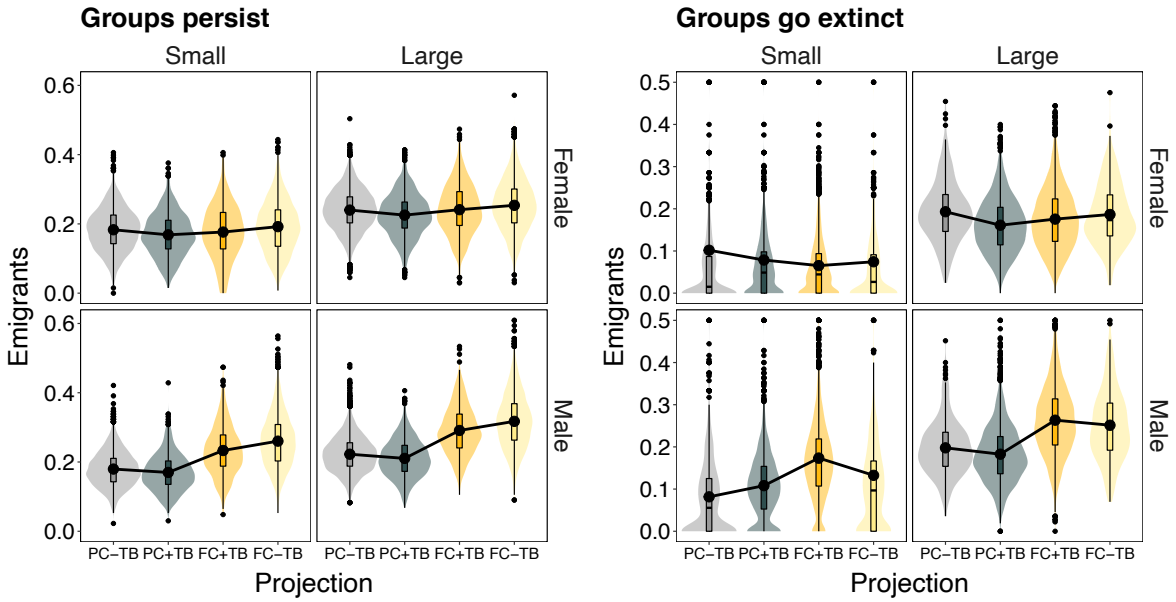

Figure S3.11. Effects of climate and clinical TB on the monthly average number of female and male emigrants. Boxplots and violin plots show the distribution for initially small and medium/large groups, across projections of the IBM where extinction did not occur vs. where it occurred after 12 years. Projections are based on four scenarios: allowing for TB (+TB) or keeping probability of clinical TB = 0 (-TB) while using observed past climate deviations (PC) in demographic models or sampling assumed future values (FC).

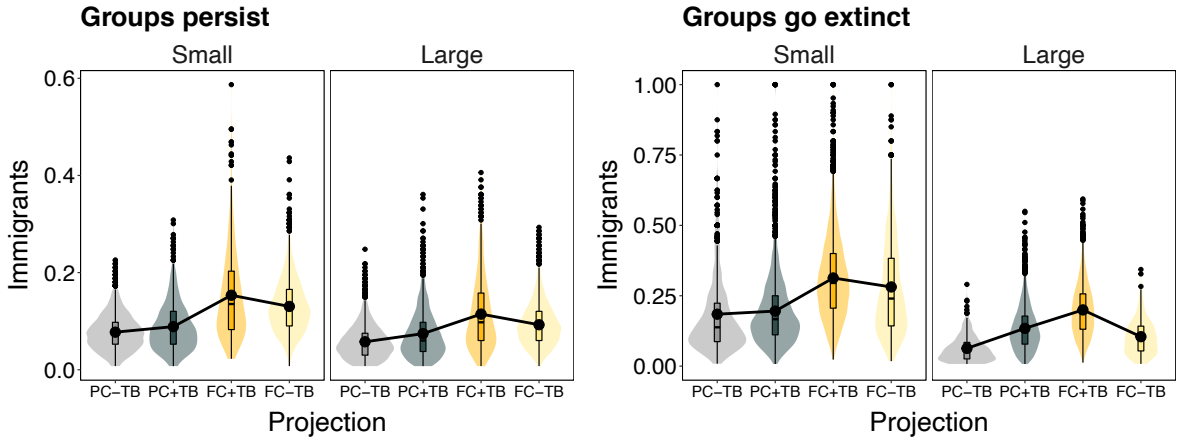

Figure S3.12. Effects of climate and clinical TB on the monthly average number of male immigrants. Boxplots and violin plots show the distribution for initially small and medium/large groups, across projections of the IBM where extinction did not occur vs. where it occurred after 12 years. Projections are based on four scenarios: allowing for TB (+TB) or keeping probability of clinical TB = 0 (-TB) while using observed past climate deviations (PC) in demographic models or sampling assumed future values (FC).

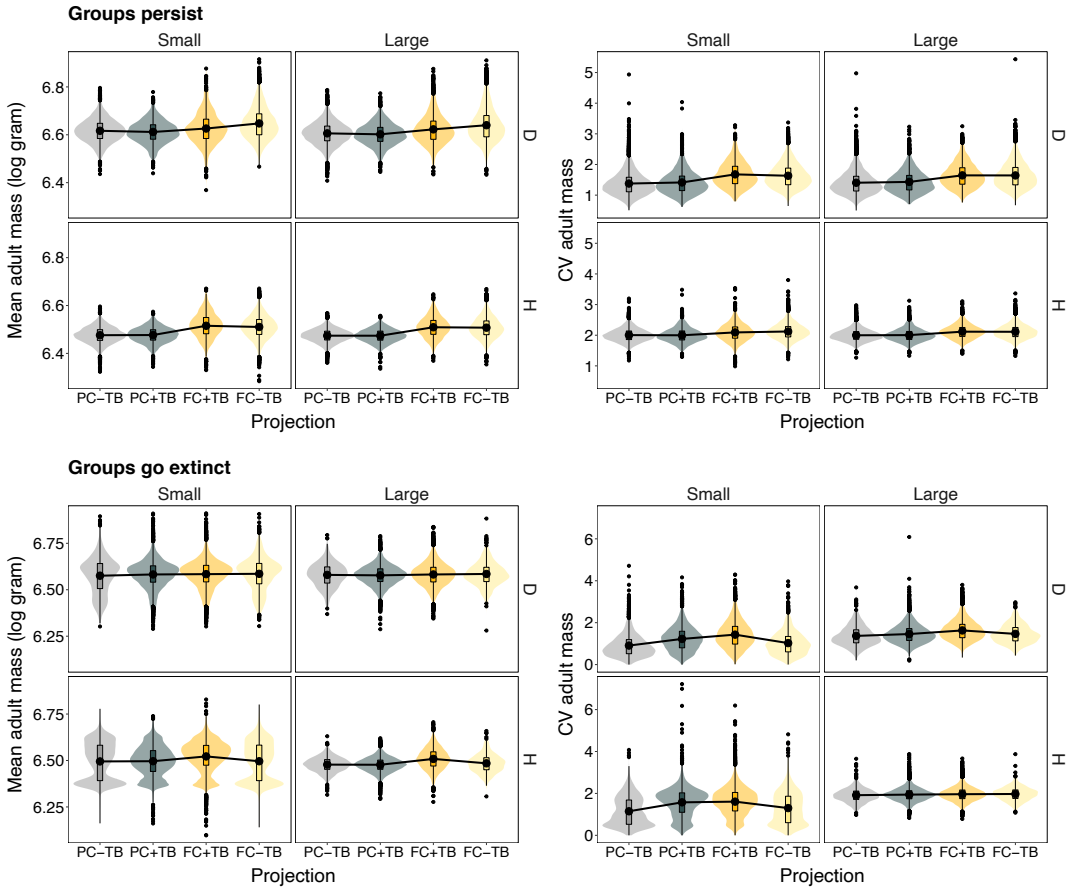

Figure S3.13. Effects of climate and clinical TB on mean and variation (CV) of mass of dominant (D) and helper (H) meerkats. Boxplots and violin plots show the distribution of mass metrics for initially small and medium/large groups, across projections of the IBM where extinction did not occur vs. where it occurred after 12 years. Projections are based on four scenarios: allowing for TB (+TB) or keeping probability of clinical TB = 0 (-TB) while using observed past climate deviations (PC) in demographic models or sampling assumed future values (FC).

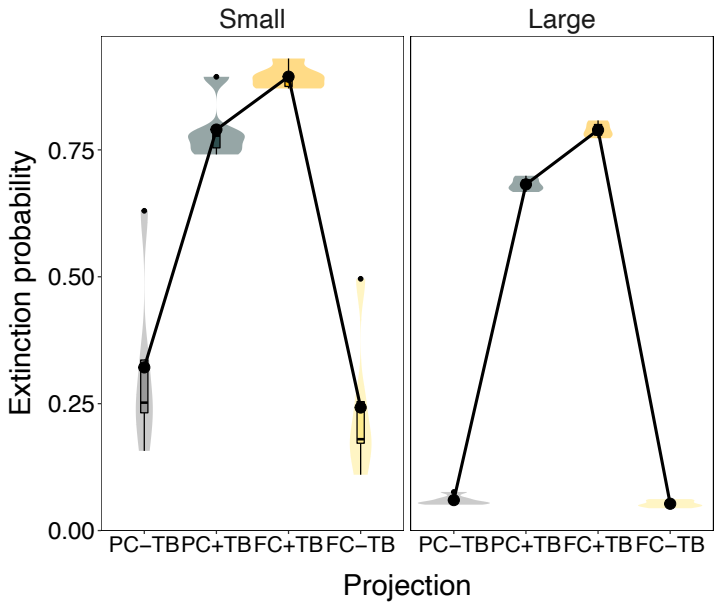

Figure S3.14. Effects of climate and TB perturbations on group extinction. Boxplots and violin plots show the distribution of extinction probabilities for initially small and medium/large groups. Projections are based on four scenarios: allowing for TB (+TB) or keeping probability of clinical TB = 0 (-TB) while using observed past climate deviations (PC) in demographic models or sampling assumed future values (FC).

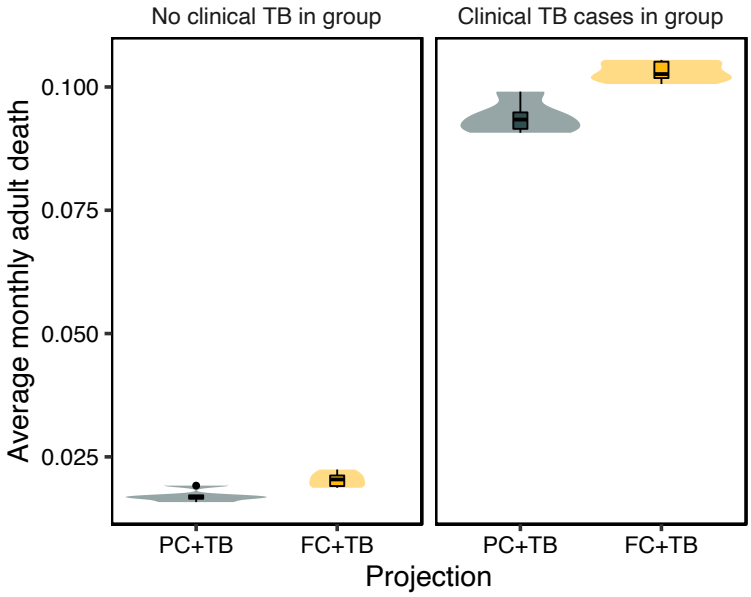

Figure S3.15. Climate change affects the demographic consequences of TB in meerkat groups. Averages were calculated as the proportion of adults dying in any given month across years. Boxplots and violin plots show the distribution of values across groups and IBM perturbations: allowing TB infection and using observed past climate deviations (PC) in demographic models or sampling assumed future values (FC) based on four climate change scenarios. Black dots connected by lines show averages.

S3.4 Demographic pathways of climate-change effects on groups

The effects of demographic rates on extinction via group size can occur because a decrease in group size in month *t* can either (a) immediately cause group extinction or (b) affect demographic rates at *t*+1, *t*+2, etc., and therefore cause delayed effects on extinction. To better understand the contribution of a delayed group-size effect on extinction, we performed IBM perturbations where we introduced temperature extremes in all demographic rates (thus accounting for correlations in demographic-rate response) and fixed group sizes at intermediate values (15 individuals) when predicting demographic rates. It has been shown that intermediate group sizes are optimal for group persistence, while both high (favouring female emigration) and particularly low (decreasing survival and reproduction) group sizes negatively affect group persistence[13,16]. We perturbed the effects of group size either after a group was TB affected, repeating the monthly TB status of the baseline IBM (as defined in the main text); or allowing clinical TB probability to change in the simulations (to assess the delayed effect of group size on this probability). We compared these perturbations to a baseline (climate change in demographic rates but group sizes not fixed).

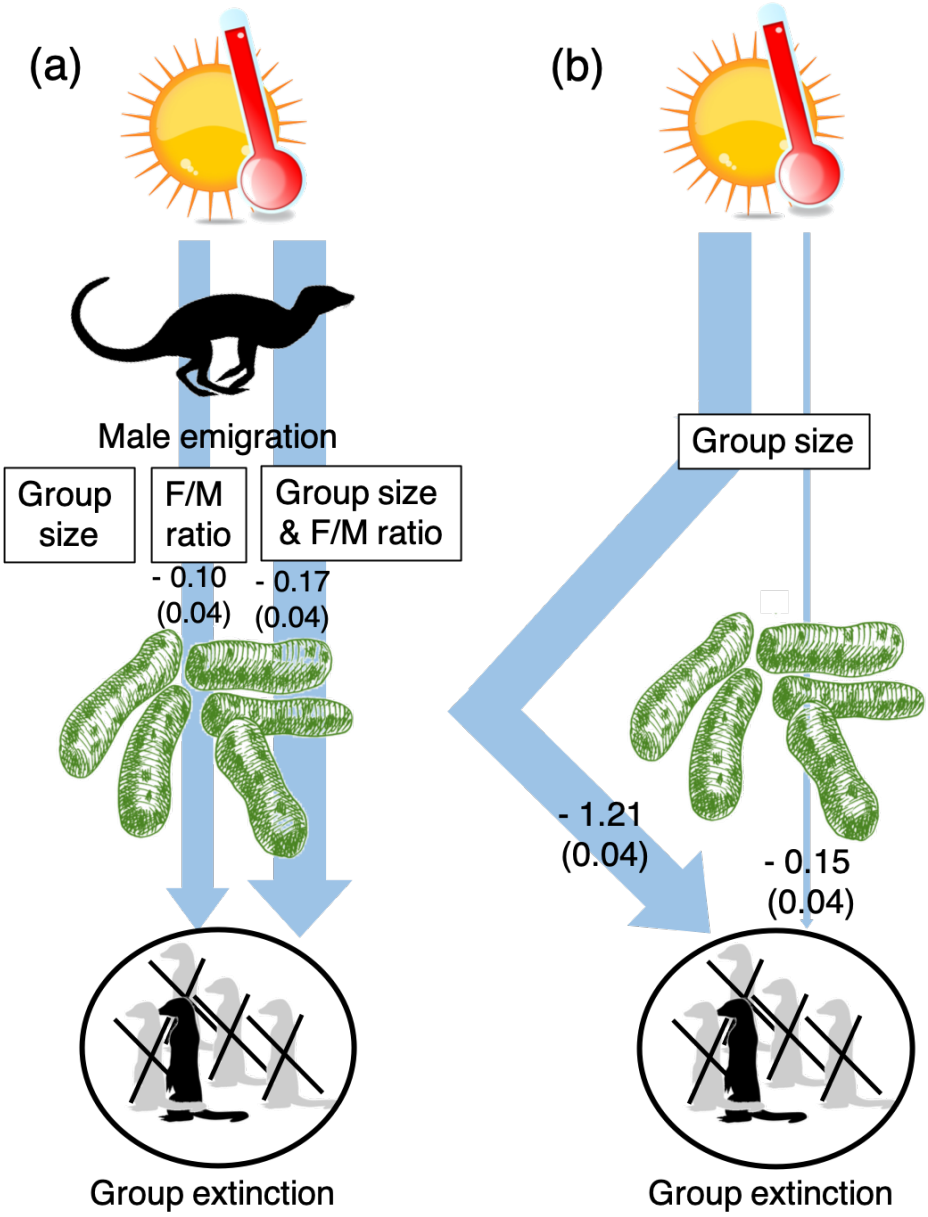

Figure S3.16. Effects of delayed group-size effects on group extinction. Arrows show decreases in the probability of quasi-extinction of groups after 12 years under different IBM perturbations. In (a), higher temperature extremes affect male emigration, which can affect group extinction by altering immigration, and hence probability of clinical TB, via changes in group size or composition. To assess the effect of the latter, group size or ratio of females (F) to males (M) were fixed at 15 and 0.5, respectively, when modelling immigration. In (b), higher temperature extremes affect all demographic rates and group sizes are fixed to 15 after groups become affected by clinical TB (no change the baseline TB occurrence) or before (allowing the probability of clinical TB affecting groups to change). Numbers show coefficients from GLMMs that compare the group-size perturbations to a baseline where higher temperature extremes affect (a) male emigration or (b) all demographic rates but group size are not fixed. Arrow size is proportional to effect size.

Table S3.3. Effects of introducing climate-change perturbations (sampling hot years 2015, 2016) to IBM submodels compared to baseline IBM simulations (sampling remaining years). Perturbations included modelling climate change in the probability of TB occurrence; and in key demographic rates without changing group clinical-TB status from the baseline IBM or allowing the probability of TB occurring in groups to change via the effect of group size on immigration (see *Methods* in main text). Effects represent fixed effects (+SE) from generalized mixed effect models (GLMMs); i.e., differences, compared to the baseline, in introducing higher temperature extremes in a given IBM submodel. Note that in Fig. 6, we plot **significant effects** (in **bold**), i.e., where the C.I., defined as mean effect ± 1.96SE, did not cross 0.

Metric	IBM submodel perturbed	Clinical-TB state fixed	Effect (+SE)
Group extinction	Female helper survival	yes	- 0.07 (0.04)
	Male helper survival	yes	- 0.08 (0.04)
	Dominant reproduction	yes	- 0.06 (0.04)
	Female helper emigration	yes	- 0.06 (0.04)
	Male helper emigration	yes	- 0.07 (0.04)
	Male immigration	yes	- 0.06 (0.04)
	Probability of clinical TB	no	**0.26 (0.04)**
	Female helper survival	no	- 0.04 (0.04)
	Male helper survival	no	- 0.01 (0.04)
	Dominant reproduction	no	- 0.06 (0.04)
	Female helper emigration	no	- 0.08 (0.04)
	Male helper emigration	no	**0.16 (0.04)**
	Male immigration	no	- 0.00 (0.04)

Supporting Material S4 - Sensitivity to male emigration

We assigned emigration, for both male and female meerkats, if an individual was observed to form roving coalitions in the month prior to disappearance. This approach has provided robust estimates of female emigration[1,13] and is based on extensive field observations, individual tracking, and expert knowledge for both sexes[8]. However, males are more mobile than females, and can disperse more spontaneously, and for 10 % of helper males, we were not certain whether individuals emigrated successfully or died. In our main analyses, we assumed these individuals died because mortality is high during dispersal events and was a more likely fate than successful emigration outside the study population. In addition, we performed sensitivity analyses of this assumption by considering (i) all uncertain cases (*Pert 1*) or (ii) those cases where males were natal to a group and were between three and five years old (*Pert 2*) (i.e., the age at which males are most likely to leave their natal group[30]) as emigrations (i.e, survival = 1 and emigration = 1). We then recalculated survival and

emigration rates for helper males, and repeated IBM projections as described in the second section of *IBM projections under increases in temperature extremes* in the main text (i.e., projecting extreme years with probability of occurrence of 0.75). Figure S.4.1 below shows that results were not sensitive to assuming death vs. emigration for the subset of the males. The only metric that shows some variation is group extinction probability for small groups. However, as other metrics do not vary, this variability can be attributed to a relatively high prevalence of stochastic extinction events in small groups.

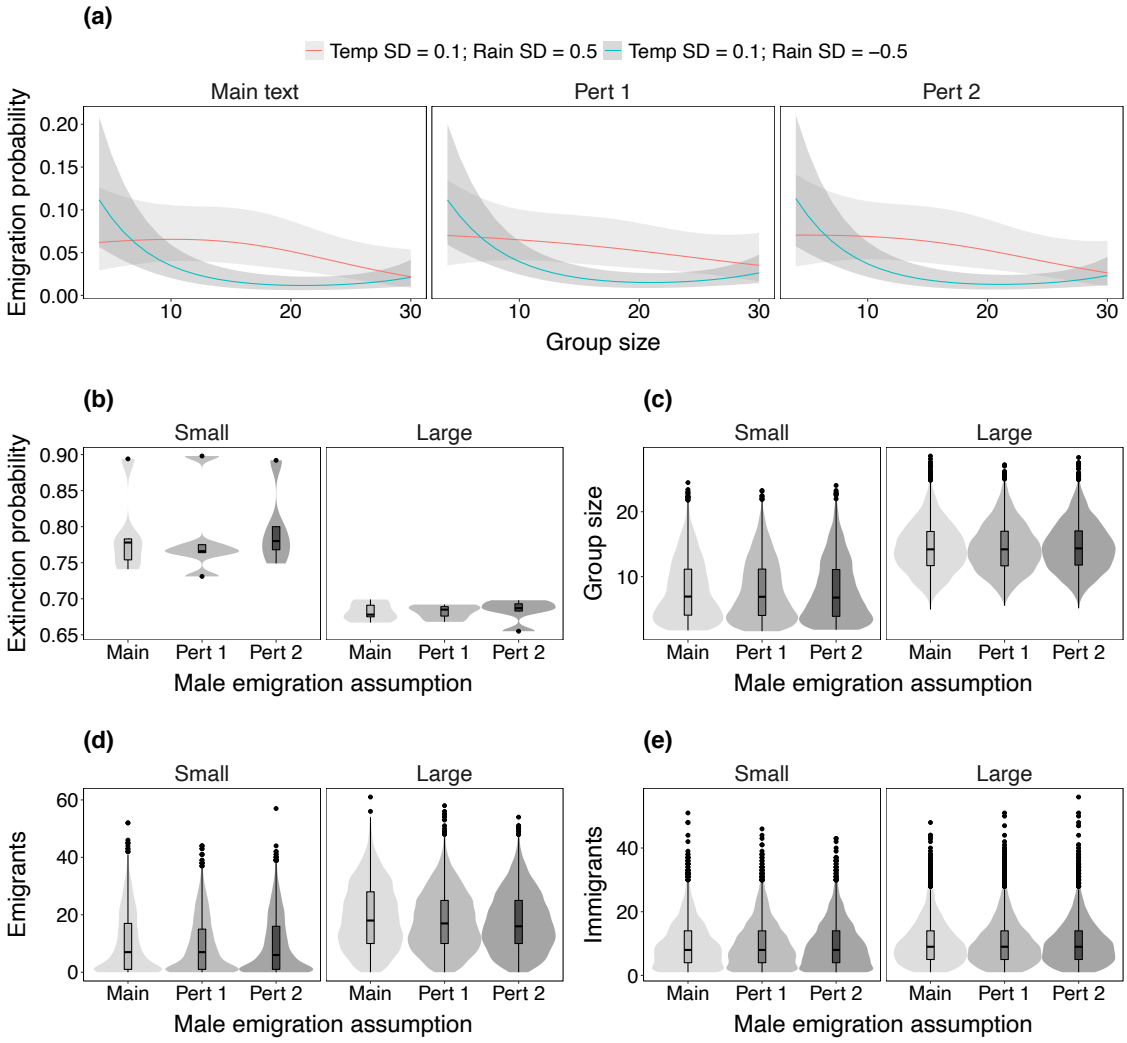

Figure S4.1. Sensitivity of modelling outputs to different underlying assumptions of male emigration. See text above for definitions of Pert 1 and Pert 2. Line and shaded areas (a) show mean predictions and the 95 % prediction interval, respectively, of GAMs, using the same constraints as described in Figure 3 in the main text. Boxplots and violin plots (b-e) show the distribution of metrics for initially small and medium/large groups, across simulations of the IBM. In (d) and (e), averages of the total numbers of emigrants and immigrants across simulations are shown.

Supporting Material S5 - Parameter uncertainty

When projecting mass and group dynamics through time using the IBM, we quantified the contribution of parameter uncertainty from the underlying demographic-rate models to these projections. We used stratified, nonparametric hierarchical bootstrapping[31] to incorporate this uncertainty into projections, which we previously successfully used in [1]. We performed 100 iterations to resample raw data within each stage and year to reflect the hierarchical model structure. For each of the 100 resampled datasets, we calculated demographic rates and used these new values to project group dynamics for 30 years using 100 simulations, randomly sapling years during each simulation. Then, to quantify how much parameter uncertainty contributed to the overall variance in output metrics, we fitted a linear mixed-effects model (LMM) using three metrics of interest as response and the bootstrap replicate as a random effect on the model mean[32] (Table S5.1). Results from the LMM show that parameter uncertainty explains little variance in the projections. This is in line with previous results projecting meerkat population dynamics using a very similar modelling approach[1].

Table S5.1. Parameter uncertainty explains little variance in the metrics of interest obtained from observed data and from projections of meerkat group dynamics for 30 years. 100 stratified bootstrap samples from three raw datasets were used to fit demographic-rate models and assess projected metrics. The proportion of variance (var) explained by parameter (P) uncertainty from these models compared to the total variance (R) was assessed with linear mixed effect models (LMMs) where the bootstrap samples were incorporated as random effect. The total number of observations in the LMMs was 10,000.

Metric	Var_P	Var_R	% Var_P
# Immigrants	0.3	3.8	8.8 %
Abundance adults	0.01	0.11	9.1 %
Body mass	0.005	0.47	1.0 %

REFERENCES

1. Paniw, M., Maag, N., Cozzi, G., Clutton-Brock, T. & Ozgul, A. Life history responses of meerkats to seasonal changes in extreme environments. *Science* **363**, 631–635 (2019).
2. Lukas, D. & Clutton-Brock, T. Climate and the distribution of cooperative breeding in mammals. *R Soc. Open Sci.* **4**, 160897 (2017).
3. Cornwallis, C. K. *et al.* Cooperation facilitates the colonization of harsh environments. *Nat. Ecol. Evol.* **1**, 57 (2017).
4. Griesser, M., Drobniak, S. M., Nakagawa, S. & Botero, C. A. Family living sets the stage for cooperative breeding and ecological resilience in birds. *PLoS Biol.* **15**, e2000483 (2017).
5. Clutton-Brock, T. H. *et al.* Costs of cooperative behaviour in suricates (*Suricata suricatta*). *Proc. Biol. Sci.* **265**, 185–190 (1998).
6. Doolan, S. P. & Macdonald, D. W. Breeding and juvenile survival among slender-tailed meerkats (*Suricata suricatta*) in the south-western Kalahari: ecological and social influences. *J. Zool.* **242**, 309–327 (1997).
7. Young, A. J. *et al.* Stress and the suppression of subordinate reproduction in cooperatively breeding meerkats. *Proc. Natl. Acad. Sci. U. S. A.* **103**, 12005–12010 (2006).
8. Maag, N., Cozzi, G., Clutton-Brock, T. & Ozgul, A. Density-dependent dispersal strategies in a cooperative breeder. *Ecology* (2018).
9. Clutton-Brock, T. H., Hodge, S. J. & Flower, T. P. Group size and the suppression of subordinate reproduction in Kalahari meerkats. *Anim. Behav.* **76**, 689–700 (2008).
10. Clutton-Brock, T. H. *et al.* Reproduction and survival of suricates (*Suricata suricatta*) in the southern Kalahari. *Afr. J. Ecol.* **37**, 69–80 (1999).
11. Van de Ven, T. M. F. N., Fuller, A. & Clutton-Brock, T. H. Effects of climate change on pup growth and survival in a cooperative mammal, the meerkat. *Funct. Ecol.* **34**, 194–202 (2020).
12. Russell, A. F. *et al.* Factors affecting pup growth and survival in co-operatively breeding meerkats Suricata suricatta. *J. Anim. Ecol.* **71**, 700–709 (2002).
13. Ozgul, A., Bateman, A. W., English, S., Coulson, T. & Clutton-Brock, T. H. Linking body mass and group dynamics in an obligate cooperative breeder. *J. Anim. Ecol.* **83**, 1357–1366 (2014).
14. Wood, S. N. *Generalized additive models: an introduction with R*. (Chapman and Hall/CRC,

2006).

15. Bartón, K. MuMIn : multi-model inference. *http://r-forge.r-project.org/projects/mumin/* (2020).
16. Bateman, A. W., Ozgul, A., Coulson, T. & Clutton-Brock, T. H. Density dependence in group dynamics of a highly social mongoose, *Suricata suricatta*. *J. Anim. Ecol.* **81**, 628–639 (2012).
17. Bateman, A. W., Ozgul, A., Nielsen, J. F., Coulson, T. & Clutton-Brock, T. H. Social structure mediates environmental effects on group size in an obligate cooperative breeder, *Suricata suricatta*. *Ecology* **94**, 587–597 (2013).
18. Grimm, V. *et al.* The ODD protocol: A review and first update. *Ecol. Model.* **221**, 2760–2768 (2010).
19. Sharp, S. P. & Clutton-Brock, T. H. Reproductive senescence in a cooperatively breeding mammal. *J. Anim. Ecol.* **79**, 176–183 (2010).
20. English, S., Bateman, A. W. & Clutton-Brock, T. H. Lifetime growth in wild meerkats: incorporating life history and environmental factors into a standard growth model. *Oecologia* **169**, 143–153 (2012).
21. Patterson, S., Drewe, J. A., Pfeiffer, D. U. & Clutton-Brock, T. H. Social and environmental factors affect tuberculosis related mortality in wild meerkats. *J. Anim. Ecol.* **86**, 442–450 (2017).
22. Clutton-Brock, T. H. & Manser, M. Meerkats: cooperative breeding in the Kalahari. *Cooperative breeding in vertebrates: Studies of ecology, evolution, and behavior* 294–317 (2016).
23. Stephens, P. A., Russell, A. F., Young, A. J., Sutherland, W. J. & Clutton-Brock, T. H. Dispersal, eviction, and conflict in meerkats (*Suricata suricatta*): an evolutionarily stable strategy model. *Am. Nat.* **165**, 120–135 (2005).
24. Clutton-Brock, T. H. *et al.* Evolution and development of sex differences in cooperative behavior in meerkats. *Science* **297**, 253–256 (2002).
25. Tredennick, A. T., Teller, B. J., Adler, P. B., Hooker, G. & Ellner, S. P. Size-by-environment interactions: a neglected dimension of species' responses to environmental variation. *Ecol. Lett.* **21**, 1757–1770 (2018).
26. Truitt, L. L., McArt, S. H., Vaughn, A. H., Ellner, S. P. Trait-based modeling of multihost pathogen transmission: Plant-pollinator networks. *Am. Nat.* **193** (2019).
27. Hansen, B. B. *et al.* More frequent extreme climate events stabilize reindeer population dynamics. *Nature Comm.* **10** (2019).

28. Sanderson, B.M., Knutti, R. & Caldwell, P. A representative democracy to reduce interdependency in a multimodel ensemble. *J. Clim*. **28**, 5171–5194 (2015).
29. Tredennick, A. T. *et al*. Forecasting climate change impacts on plant populations over large spatial extents. *Ecosphere* **7**, e01525 (2016).
30. Spong, G. F., Hodge, S. J., Young, A. J. & Clutton-Brock, T. H. Factors affecting the reproductive success of dominant male meerkats. *Mol. Ecol.* **17**, 2287–2299 (2008).
31. Davison, A. C. & Hinkley, D. V. *Bootstrap Methods and Their Application*. (Cambridge University Press, 1997).
32. Paniw, M., Quintana-Ascencio, P. F., Ojeda, F. & Salguero-Gómez, R. Accounting for uncertainty in dormant life stages in stochastic demographic models. *Oikos* **126**, 900–909 (2017).